iScience

CellPress
OPEN ACCESS

Article

Involvement of Mrgprd-expressing nociceptors-recruited spinal mechanisms in nerve injury-induced mechanical allodynia

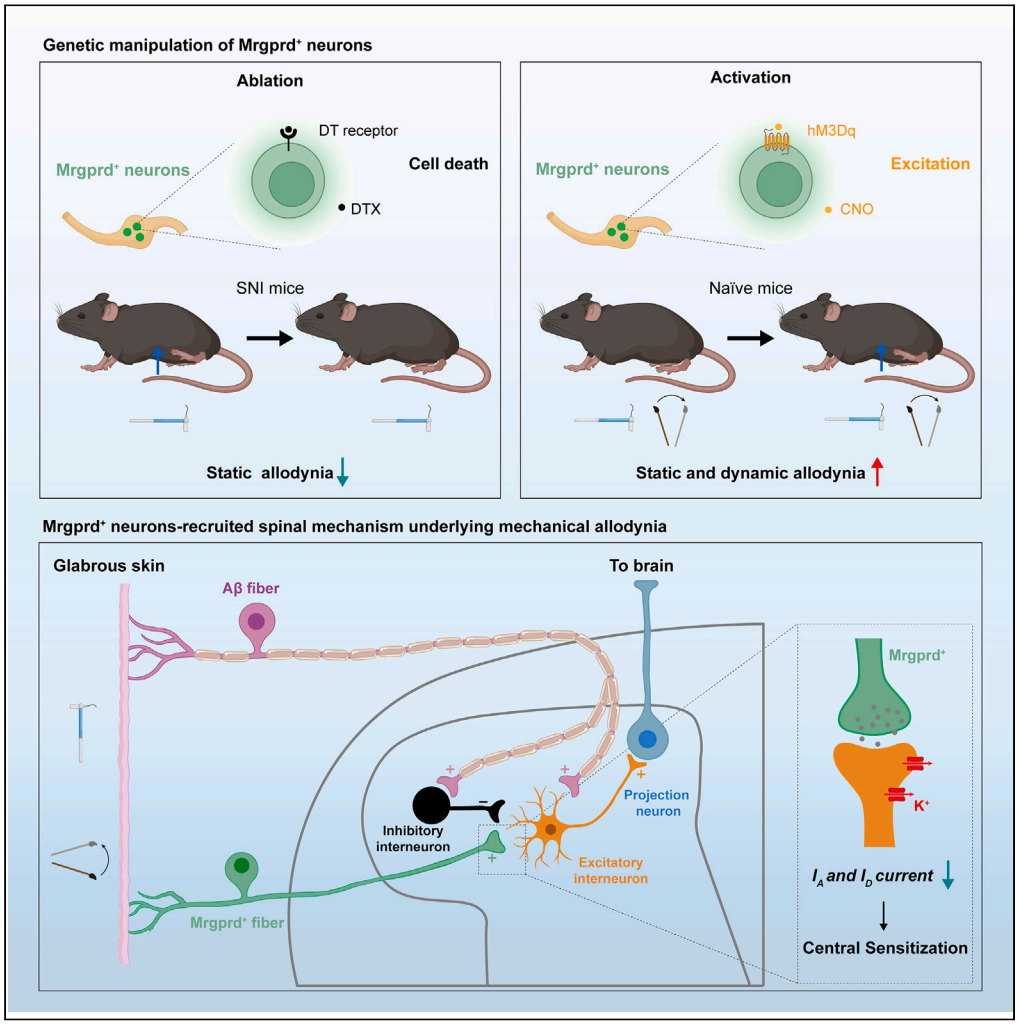

Liangbiao Wang, Xiaojing Su, Jinjin Yan, ..., Wei Hu, Xinfeng Liu, Yan Zhang

andinghu@ustc.edu.cn (W.H.)
xfliu2@ustc.edu.cn (X.F.L.)
yzhang19@ustc.edu.cn (Y.Z.)

Highlights

Mrgprd$^+$ neurons ablation selectively attenuates static allodynia after nerve injury

Mrgprd$^+$ neurons ablation partly "closes" nerve injury-opened Aβ inputs pathway

Priming Mrgprd$^+$ neurons activation induces allodynia and "opens" Aβ pathway

Mrgprd$^+$ inputs attenuate I_A/I_D of $_v$II$_i$ neurons with convergent input from Aβ fibers

Wang et al., iScience 26, 106764
May 19, 2023
https://doi.org/10.1016/j.isci.2023.106764

iScience

CellPress
OPEN ACCESS

Article

Involvement of Mrgprd-expressing nociceptors-recruited spinal mechanisms in nerve injury-induced mechanical allodynia

Liangbiao Wang,[1,4] Xiaojing Su,[1,4] Jinjin Yan,[1] Qiaofeng Wu,[1] Xiang Xu,[1] Xinyue Wang,[1] Xiaoqing Liu,[2] Xiaoyuan Song,[3] Zhi Zhang,[3] Wei Hu,[1,*] Xinfeng Liu,[1,*] and Yan Zhang[1,5,*]

SUMMARY

Mechanical allodynia and hyperalgesia are intractable symptoms lacking effective clinical treatments in patients with neuropathic pain. However, whether and how mechanically responsive non-peptidergic nociceptors are involved remains elusive. Here, we showed that von Frey-evoked static allodynia and aversion, along with mechanical hyperalgesia after spared nerve injury (SNI) were reduced by ablation of *Mrgprd*^{CreERT2}-marked neurons. Electrophysiological recordings revealed that SNI-opened Aβ-fiber inputs to laminae I-II$_o$ and $_v$II$_i$, as well as C-fiber inputs to $_v$II$_i$, were all attenuated in Mrgprd-ablated mice. In addition, priming chemogenetic or optogenetic activation of Mrgprd$^+$ neurons drove mechanical allodynia and aversion to low-threshold mechanical stimuli, along with mechanical hyperalgesia. Mechanistically, gated Aβ and C inputs to $_v$II$_i$ were opened, potentially via central sensitization by dampening potassium currents. Altogether, we uncovered the involvement of Mrgprd$^+$ nociceptors in nerve injury-induced mechanical pain and dissected the underlying spinal mechanisms, thus providing insights into potential therapeutic targets for pain management.

INTRODUCTION

Acute pain is beneficial for warning the body to avoid further tissue injury from external noxious stimuli. Nonetheless, chronic neuropathic pain is maladaptive,[1] and causes both physical and mental impairment. Two prominent hallmarks in neuropathic pain patients are mechanical allodynia whereby innocuous touch evokes severe pain, and hyperalgesia whereby noxious stimuli evoke increased pain.[2] Unfortunately, these most common symptoms lack effective clinical management without strong adverse effects, such as nausea, tolerance, and dependence.[3] Thus, it's imperative to obtain a deep understanding of the mechanisms underlying neuropathic pain for exploring new analgesic targets.

The spinal cord is the first relay station for multiple somatosensation processing, including pain. The gate control theory (GCT) proposed by Melzack and Wall in 1965 suggests that pain-transmitting (T) neurons in the dorsal spinal cord receive convergent inputs from low-threshold mechanoreceptors (LTMRs) and noxious nociceptors.[4] Tactile stimuli normally cannot excite T neurons and evoke pain due to concurrent feedforward activation of "gate-keeper" inhibitory interneurons (INs). Under pathological conditions, gated LTMR inputs to T neurons are "opened", thereby developing mechanical allodynia. In the past few years, multiple studies investigated the contribution of INs inactivation along with T neurons sensitization to mechanical hypersensitivity in neuropathic pain.[5,6] However, the role of nociceptors in neuropathic pain has been largely neglected, especially for Mas-related G protein-coupled receptor subtype D (Mrgprd)-expressing nociceptors which respond to innocuous punctate stimuli.[7]

The expression of *Mrgprd* is regulated by the *Runx1* gene, and the majority (~90%) is *Runx1*-persistent.[8] It has been identified as a marker of non-peptidergic nociceptors expressing isolectin B4 (IB4)[9] and shows dynamic expression when *Mrgprd* is expressed more broadly on *Mrgpra3*, *Mrgprb4*, and *Somatostatin*-positive dorsal root ganglia (DRG) neurons in early development than in adulthood.[10–12] Previous studies showed that Mrgprd$^+$ neurons are required for full expression of mechanical hypersensitivity in inflammatory pain.[13–15] To date, the role of Mrgprd$^+$ nociceptors in neuropathic pain remains controversial. An early study reported that mice with genetic ablation of Na$_v$1.8-expressing nociceptors, which include Mrgprd$^+$

[1]Department of Neurology, the First Affiliated Hospital of USTC, Division of Life Sciences and Medicine, University of Science and Technology of China, Hefei, Anhui 230001, China

[2]School of Basic Medical Sciences, Division of Life Sciences and Medicine, University of Science and Technology of China, Hefei, Anhui 230026, China

[3]Hefei National Laboratory for Physical Sciences at the Microscale, CAS Key Laboratory of Brain Function and Disease, School of Life Sciences, Division of Life Sciences and Medicine, University of Science and Technology of China, Hefei, Anhui 230026, China

[4]These authors contributed equally

[5]Lead contact

*Correspondence: andinghu@ustc.edu.cn (W.H.), xfliu2@ustc.edu.cn (X.F.L.), yzhang19@ustc.edu.cn (Y.Z.)

https://doi.org/10.1016/j.isci.2023.106764

neurons, showed no deficits in mechanical hypersensitivity after nerve injury.[13] In contrast, a recent study using Mrgprd-knockout mice concluded that Mrgprd$^+$ neurons were necessary for the initiation of mechanical hypersensitivity in neuropathic pain.[16] Nevertheless, constitutive loss of $Na_v1.8^+$ or Mrgprd$^+$ neurons from the embryonic stage could allow compensation by other populations of sensory neurons and brings difficulty in unbiased interpretation. In a gain-of-function study, Warwick *et al.* showed that optical activation of *Mrgprd*^{Cre} lineage neurons can drive aversion which is absent in normal mice,[11,17] and by extension, pain after nerve injury.[12] Of note, *Mrgprd* knock-in mouse line captures all transient Mrgprd$^+$ populations including Mrgpra3-expressing-C afferents which are known to evoke nocifensive responses following optical stimulations.[18] Thus, the exact role of persistent Mrgprd$^+$ neurons in neuropathic pain is still ambiguous. Our recent work showed that adult Mrgprd$^+$ nociceptors were involved in neuropathic pain.[19] However, the underlying spinal mechanism of how Mrgprd$^+$ neurons are involved in neuropathic pain remains unknown.

In this study, by using a tamoxifen-inducible *Mrgprd*^{CreERT2} mouse line, we specifically targeted the adult Mrgprd-expressing neurons to systematically assess their role in neuropathic pain and the underlying spinal mechanisms. We first showed that ablation of *Mrgprd*^{CreERT2}-marked neurons selectively attenuates nerve injury-induced punctate hypersensitivity (static allodynia), but not brush-evoked mechanical hypersensitivity (dynamic allodynia). Mechanistically, the gated Aβ-fiber inputs to superficial laminae (I–II$_o$) and ventral inner laminae II ($_v$II$_i$) were both opened by nerve injury, and the opened Aβ pathways were attenuated by Mrgprd$^+$ neurons ablation. Meanwhile, we showed that von Frey-evoked mechanical hyperalgesia after SNI was compromised in mice with *Mrgprd* ablation, largely due to the blockage of opened C-fiber inputs to $_v$II$_i$ neurons upon SNI. In contrast, priming chemogenetic or optogenetic stimulation of *Mrgprd*^{CreERT2}-marked neurons led to both static and dynamic allodynia, as well as an aversion to innocuous mechanical stimuli. Finally, we showed that Mrgprd$^+$ inputs opened Aβ and C input pathways in laminae $_v$II$_i$, potentially via central sensitization rather than disinhibition. Collectively, our study reveals spinal mechanisms of how Mrgprd$^+$ sensory neurons are involved in nerve injury-induced mechanical allodynia and hyperalgesia, which will benefit the identification of therapeutic targets to treat neuropathic pain.

RESULTS

Attenuated static allodynia following nerve injury in Mrgprd-ablated mice

To investigate the role of the adult Mrgprd$^+$ nociceptors in the development of neuropathic pain, we examined how nerve injury-induced mechanical and thermal hypersensitivity were affected by ablating Mrgprd$^+$ sensory neurons. To achieve this, we crossed *Mrgprd*^{CreERT2} mice with *ROSA26*^{iDTR} mice to generate a heterozygous *Mrgprd*^{CreERT2}; *ROSA26*^{iDTR} (also referred to as *Mrgprd*^{CreERT2}*-DTR*) strain. By injecting the tamoxifen at postnatal 21 days (P21), the expression of the Diphtheria toxin receptor (DTR) was specifically induced in adult Mrgprd$^+$ sensory neurons.[11,20] Next, we administrated the diphtheria toxin (DTX) at P42, then performed SNI or assessed the ablation efficiency at 3 weeks afterward (Figure 1A). By performing *in situ* hybridization (ISH) and immunofluorescence in the DRG, we revealed that ~92% of Mrgprd$^+$ sensory neurons (Figures 1B and 1C), and ~29% of total DRG neurons were eliminated (Figure S1A). The number of other groups of DRG neurons, including NF200$^+$, TH$^+$, and CGRP$^+$ cells, was unaffected (Figures S1B–S1D) indicating the ablation specificity. We refer to these *Mrgprd*^{CreERT2}; *ROSA26*^{iDTR} mice as Mrgprd-ablated mice. They displayed reduced sensitivity to von Frey filament-evoked punctate mechanical stimulation (Figure 1D), but normal responses to brush-evoked dynamic mechanical stimulation and nociceptive thermal stimulation (Figures 1E and 1F). After nerve injury, a well-established model of peripheral neuropathic pain,[21] Mrgprd-ablated mice displayed attenuation of filament-evoked static allodynia (Figure 1D). However, the extent of brush-evoked dynamic allodynia and thermal hypersensitivity was unaffected (Figures 1E and 1F).

In addition, we examined how established mechanical and thermal hypersensitivity in SNI mice were affected after the ablation of Mrgprd$^+$ neurons. Similarly, static allodynia was selectively reduced (Figure 1G), while dynamic allodynia and thermal hypersensitivity were unchanged (Figures 1H and 1I). Taken together, Mrgprd$^+$ neurons are required for both the development and maintenance of static allodynia in neuropathic pain.

Loss of punctate stimuli-evoked aversion following nerve injury in Mrgprd-ablated mice

To further assess the requirement of Mrgprd$^+$ nociceptors for static allodynia, we examined the expression of spinal dorsal horn c-Fos, a classical neuronal activity marker (Figure 2A). In sham control mice, rare c-Fos

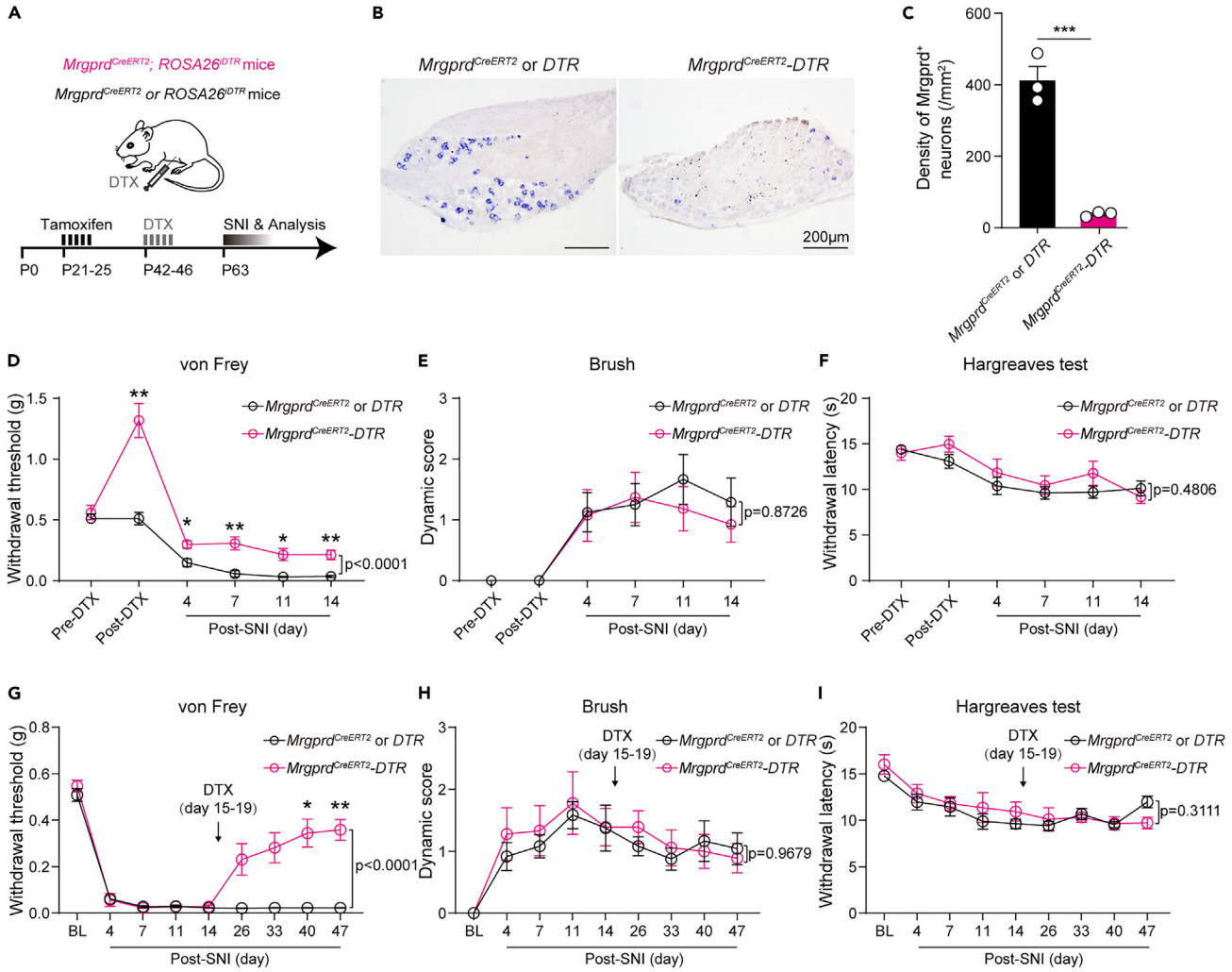

Figure 1. Attenuated static allodynia following nerve injury in Mrgprd-ablated mice

(A) An outline of the experimental scheme for tamoxifen treatment (i.p. 75 mg/kg tamoxifen per day, P21–P25), DTX treatment (i.p. 20 μg/kg, P42–P46), and morphological or behavioral analysis (starting at P63) in *Mrgprd*^{CreERT2}; *ROSA26*^{iDTR} mice.

(B and C) Representative images of *in situ* hybridization on DRG sections and statistical data for the number of Mrgprd^{+} neurons per section from control mice ("*Mrgprd*^{CreERT2} or *DTR*") and Mrgprd-ablated mice ("*Mrgprd*^{CreERT2}*-DTR*") (n = 3 animals per group, 3 sections/animal). Scale bar, 200 μm.

(D–F) Changes in von Frey filament-evoked mechanical hypersensitivity (D), brush-evoked dynamic hypersensitivity (E), and thermal hypersensitivity (F) after sequential DTX injection and SNI operation (*Mrgprd*^{CreERT2} or *DTR* group, n = 8 mice, *Mrgprd*^{CreERT2}*-DTR* group, n = 9 mice).

(G–I) Changes in von Frey filament-evoked mechanical hypersensitivity (G), brush-evoked dynamic hypersensitivity (H), and thermal hypersensitivity (I) after sequential SNI operation and DTX injection (*Mrgprd*^{CreERT2} or *DTR* group, n = 8 mice, *Mrgprd*^{CreERT2}*-DTR* group, n = 6 mice). Data are presented as mean ± SEM. *p < 0.05, **p < 0.01, ***p < 0.001. Unpaired Student's two-tailed t test for (C); Two-way repeated-measures ANOVA with holm-sidak test for (D)–(I). See also Figure S1.

expression was induced following ipsilateral hindpaw stimulation by low-threshold von Frey (0.16 g) filament (Figures 2B and 2C). After SNI, the same stimuli induced c-Fos expression in both laminae I–II and III–V of the dorsal horn (Figures 2B and 2C). However, the number of c-Fos^{+} neurons was dramatically reduced in Mrgprd-ablated SNI mice (Figures 2B and 2C).

Aversion is commonly envisioned as an affective dimension of pain.[22–24] To investigate the affective aspects of static and dynamic allodynia, we used the two-chamber, real-time place avoidance (RTPA) assay, a highly sensitive model for measuring aversive memory (Figures 2D and 2F). Compared to the sham controls, both von Frey filament (0.16 g) and light brush in SNI mice were capable of evoking robust RTPA (Figures 2E and 2G). However, von Frey-evoked RTPA was selectively abolished by ablating Mrgprd^{+}

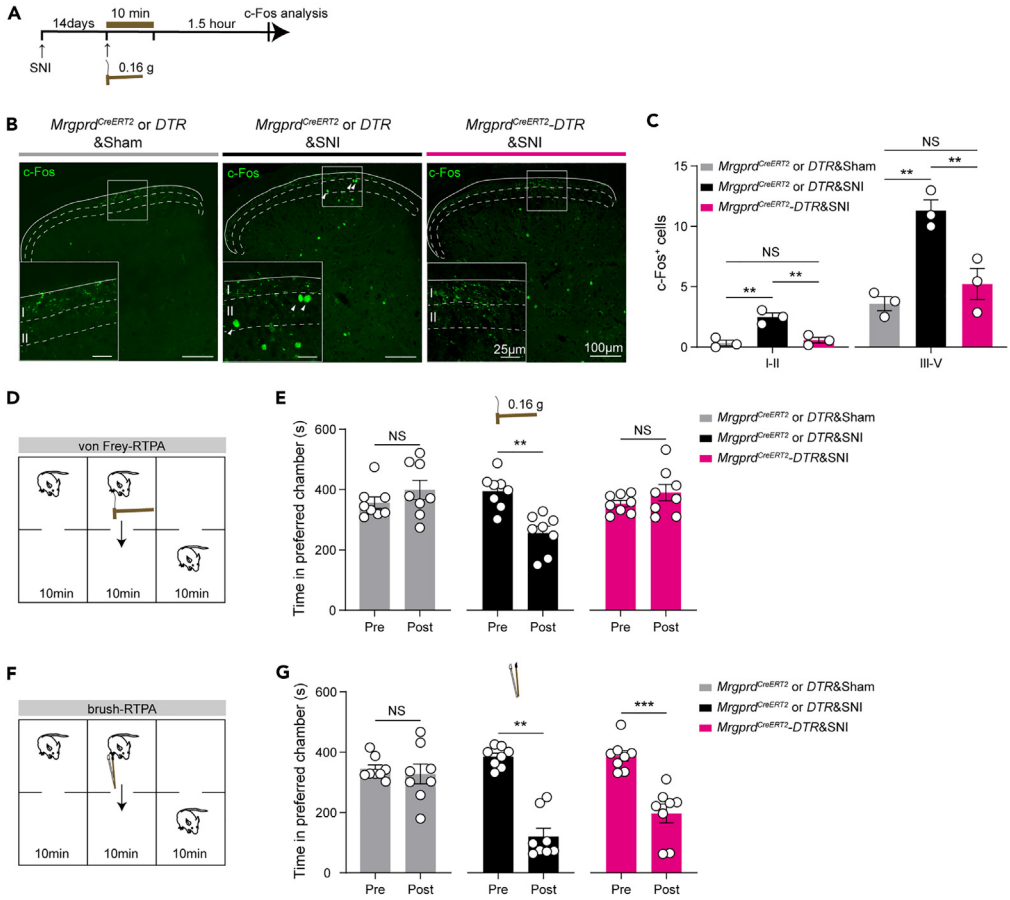

Figure 2. Attenuation of von Frey-induced c-Fos expression and loss of von Frey-evoked RTPA in Mrgprd-ablated mice with SNI

(A) An outline of the experimental scheme for c-Fos induction by 0.16 g von Frey filament (postoperative day 14).

(B and C) Representative images (B) and statistical data for c-Fos$^+$ neurons within laminae I–II and III–V of the spinal cord (C) in *Mrgprd*^{CreERT2} or *DTR*&Sham, *Mrgprd*^{CreERT2} or *DTR*&SNI, and *Mrgprd*^{CreERT2}-*DTR*&SNI mice (n = 3 mice per group, 3 sections/animal). Scale bar, 100 μm (25 μm for high magnification).

(D) Schematics of the von Frey-evoked RTPA apparatus and experimental design.

(E) Loss of 0.16 g von Frey-evoked RTPA in mice with SNI following the ablation of Mrgprd$^+$ neurons. (n = 8 mice per group).

(F) Schematics of the brush-evoked RTPA apparatus and experimental design.

(G) Brush-evoked RTPA in mice with SNI remained intact following the ablation of Mrgprd$^+$ neurons. (n = 8 mice per group). Data are presented as mean ± SEM. "NS", no significance; **p < 0.01, ***p < 0.001. One-way ANOVA with holm-sidak test for (C); Paired Student's two-tailed t test or Wilcoxon signed-rank test for (E) and (G).

neurons (Figures 2E and 2G). Taken together, Mrgprd$^+$ neurons are preferentially required for SNI-induced punctate hypersensitivity and the process of affective aspects of hypersensitive mechanical pain.

Gated Aβ-fiber inputs pathway is opened by nerve injury and attenuated following the ablation of Mrgprd$^+$ neurons

We went further to explore the neural substrates underlying attenuated static allodynia after the ablation of Mrgprd$^+$ neurons. To assess the potential involvement of SNI-sensitized Mrgprd$^+$ afferents in transmitting mechanical allodynia, we first examined the excitability of Mrgprd$^+$ neurons in naïve and SNI mice and detected no difference (Figure S2). We thus assume the involvement of touch-sensing Aβ-fibers which mediate allodynia in humans.[25–27] When mechanical allodynia develops, Aβ inputs are usually relayed from deep laminae to superficial laminae (I–II$_o$) via polysynaptic pathway.[28–30] Next, we tested whether this superficial Aβ pathway was affected by Mrgprd$^+$ neurons ablation.

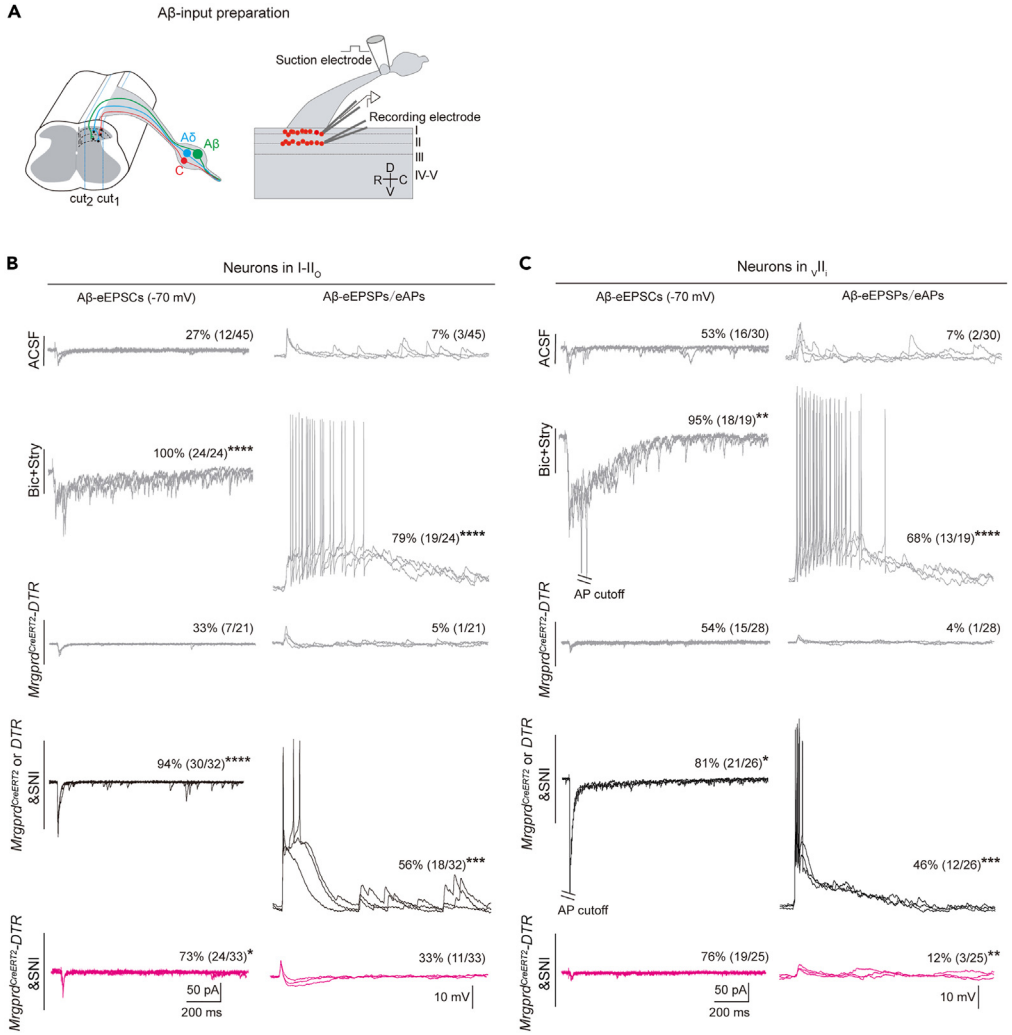

Figure 3. The gated Aβ-fiber inputs pathway is opened by nerve injury and attenuated following the ablation of *Mrgprd*^{CreERT2}-marked neurons

(A) Schematic drawing of the cutting method for parasagittal Aβ-input preparation (left) and recorded neurons (right). (B and C) Representative traces of Aβ-evoked inputs (left) and outputs (right) of the neurons in laminae I–II$_o$ (B) and laminae $_v$II$_i$ (C) from naïve control mice either with normal ACSF (top, "ACSF") or with ACSF containing bicuculline (10 μM) plus strychnine (2 μM) ("Bic+stry" group), Mrgprd-ablated mice ("*Mrgprd*^{CreERT2}-*DTR*" group), Mrgprd-ablation control mice with SNI ("*Mrgprd*^{CreERT2} or *DTR*&SNI" group), and Mrgprd-ablated mice with SNI (bottom, "*Mrgprd*^{CreERT2}-*DTR*&SNI"). Aβ inputs indicated by Aβ-eEPSCs at -70 mV with voltage-clamp; Aβ outputs indicated by Aβ-eEPSPs/eAPs with current-clamp. Data for (B) and (C) are presented as percentage. *p < 0.05, **p < 0.01, ***p < 0.001, ****p < 0.0001. Chi-square test for (B) and (C). See also Figures S2 and S3.

To this end, dorsal root-attached spinal cord slices with intact Aβ inputs were prepared. Whole-cell patch-clamp recordings were performed on neurons of laminae I–II$_o$ (Figure 3A) where pain output projection neurons are most abundant.[31] In naïve control mice, voltage-clamp recordings with holding potential at -70 mV showed that 27% (12 of 45) of I–II$_o$ neurons produced small Aβ-evoked excitatory postsynaptic currents (Aβ-eEPSCs) following dorsal root electric stimulation at 25 μA intensity which specifically recruits Aβ afferents.[29] To facilitate the recording of evoked inhibitory postsynaptic currents (eIPSCs), the membrane potential was clamped at -45 mV and 38% (10 of 26) of neurons displayed Aβ-eIPSCs, indicating the existence of feedforward inhibitory inputs to I–II$_o$ neurons. We then used the current-clamp recording to measure the synaptic output of I–II$_o$ neurons, by assessing the ability of excitatory postsynaptic potentials (EPSPs) to fire action potential (AP). Aβ-fibers stimulation failed to evoke AP firing in 93% (42 of 45) of I–II$_o$ neurons (Figure 3B). To determine if the failure of AP firing was resulting from feedforward inhibition,

recordings were performed in the disinhibition conditions by adding bicuculline (10 μM) and strychnine (2 μM) into ACSF which blocks inhibitory $GABA_A$ receptors and glycine receptors, respectively. We found 100% (24 of 24) of I–II_o neurons displayed Aβ-eEPSCs, and 79% (19 of 24) of neurons fired APs in comparison with 7% under normal ACSF (Chi-square test, $p < 0.0001$) (Figure 3B).

In consistent with morphological result (Figure S1D), Mrgprd-ablation did not change the percentage of I-II_o neurons with Aβ-eEPSCs and Aβ-eAPs: 33% (7 of 21) vs. 27% (12 of 45, Chi-square test, $p = 0.5748$), and 5% (1 of 21) vs. 7% (3 of 45, Chi-square test, $p > 0.9999$) in Mrgprd-ablated mice versus naïve control mice, respectively (Figure 3B). Next, we analyzed Aβ-fiber inputs to I–II_o neurons under neuropathic conditions. After SNI, we observed a significant increase in the percentage of neurons displaying Aβ-eEPSCs and Aβ-eAPs: 94% (30 of 32) vs. 27% (12 of 45, Chi-square test, $p < 0.0001$), and 56% (18 of 32) vs. 7% (3 of 45, Chi-square test, $p < 0.001$) in *Mrgprd*^{CreERT2} or *DTR* mice versus naïve control mice, respectively (Figure 3B). These results suggested that the gated superficial Aβ pathway was opened by peripheral nerve injury. However, in Mrgprd-ablated mice with SNI, the increased percentage of neurons displaying Aβ-eEPSCs and Aβ-eAPs was significantly reduced to 73% (24 of 33, Chi-square test, $p < 0.05$) and 33% (11 of 33, Chi-square test, $p = 0.063$), respectively (Figure 3B). Correspondingly, the amplitude of Aβ-eEPSCs was reduced (Figure S3A).

From our previous data, c-Fos expression in the deeper laminae with *Mrgprd* ablation was also decreased, potentially suggesting a ventrally directed influence on the mechanical allodynia pathway. Next, we assessed laminae $_{v}II_i$ neurons that are located nearby central terminals of Mrgprd$^+$ nociceptors[14] and relay Aβ inputs to superficial neurons.[28,29] Similar to superficial Aβ inputs pathway, Aβ inputs to $_{v}II_i$ neurons were not changed by Mrgprd$^+$ neurons ablation, and they were also gated and opened by either spinal pharmacological disinhibition or peripheral nerve injury (Figure 3C). Importantly, the increased Aβ-eAPs after SNI showed a profound reduction with *Mrgprd* ablation: from 46% (12 of 26) to 12% (3 of 25, Chi-square test, $p < 0.01$) in control and Mrgprd-ablated mice, respectively (Figure 3C). Correspondingly, the amplitude of Aβ-eEPSCs of neurons was also reduced (Figure S3B). To summarize, ablation of Mrgprd$^+$ sensory neurons inhibits the "opening" of the gated Aβ-fiber inputs pathway which serves as the substrate for transmitting mechanical hypersensitivity caused by SNI.

Impaired mechanical hyperalgesia and C-fiber inputs to $_{v}II_i$ neurons after nerve injury in Mrgprd-ablated mice

Mechanical hyperalgesia is defined as aggravated pain in response to noxious mechanical stimuli. It's another thorny syndrome besides allodynia in neuropathic pain patients. We next tested whether the behavioral responses to high-threshold mechanical stimuli (e.g. 1.0 g von Frey filament) after SNI were affected by Mrgprd$^+$ neurons ablation. In naïve conditions, mice displayed mostly paw-lifting responses following 10 trials of stimuli (data not shown). After nerve injury, the same mechanical force produced lots of delayed paw fluttering responses, a sign of mechanical hyperalgesia,[32,33] which were substantially reduced in Mrgprd-ablated mice (Figure 4A).

Given that hyperalgesia was correlated with C-fiber nociceptors and modulation of neural transmission in the spinal cord,[34] we examined how C-fiber inputs and outputs were affected to evaluate the potential spinal substrate for paw fluttering. To avoid masking C inputs by Aβ inputs, we used a modified spinal slice preparation termed "C-input preparation", in which low-threshold Aβ inputs that mostly enter the dorsal horn via dorsal funiculus were predominantly removed[28,35] (Figure S4A). We recorded neurons in the laminae $_{v}II_i$. The success of Aβ inputs cutoff was proved by the absence of Aβ-eEPSCs in 100% (11 of 11) of recorded neurons under the normal ACSF conditions and 100% (20 of 20) of neurons even under the disinhibition conditions (Figure S4B). In C-input preparation of naïve control mice, 84% (21 of 25) of neurons within $_{v}II_i$ produced detectable EPSCs following C intensity stimulations (500 μA, 0.1 ms), with only 4% (1/25) of neurons firing AP (Figure 4B). By holding the membrane potential at -45 mV, 72% (18 of 25) neurons displayed C-eIPSCs, suggesting the presence of feedforward inhibition (Figure 4B). In the presence of bicuculline and strychnine that mimics the spinal disinhibition, 92% (22 of 24) of neurons can now fire C-eAPs compared with 4% under normal ACSF (Chi-square test, $p < 0.0001$) (Figure 4B). These results support the existence of the gated C-fibers pathway in $_{v}II_i$.

We also assessed C-fiber inputs to $_{v}II_i$ neurons in intact Mrgprd-ablated mice, and they did not demonstrate any changes compared with naïve control mice (Figure 4B). Next, we analyzed C-fiber inputs to $_{v}II_i$

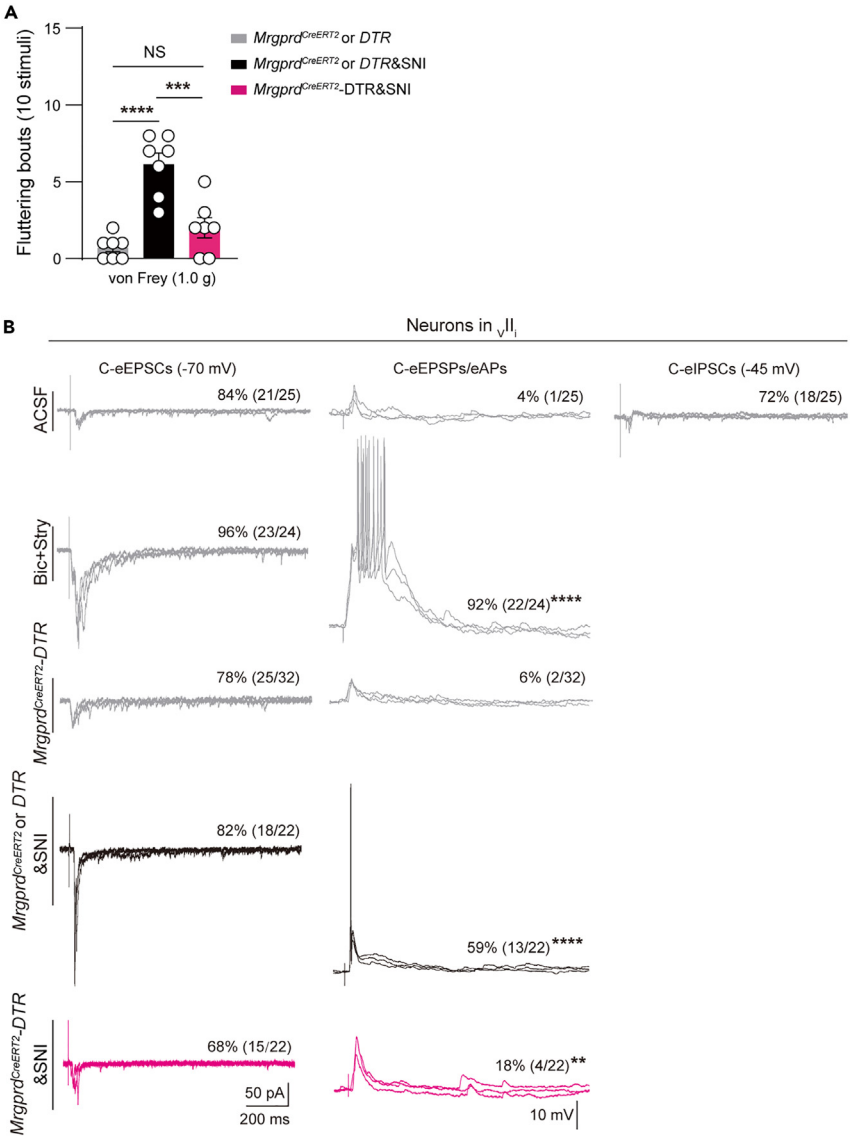

Figure 4. Impaired high-threshold mechanical force-evoked paw fluttering and C-fiber inputs to $_{v}II_{i}$ neurons after nerve injury in Mrgprd-ablated mice

(A) Paw fluttering bouts in response to 10 trials of 1.0 g von Frey paw stimulation in intact Mrgprd-ablation control mice ("*Mrgprd*^{CreERT2} or DTR"), Mrgprd-ablation control mice with SNI ("*Mrgprd*^{CreERT2} or *DTR*&SNI"), and Mrgprd-ablated mice with SNI ("*Mrgprd*^{CreERT2}-*DTR*&SNI").

(B) Representative traces of C-evoked inputs (left) and outputs (right) of the neurons in laminae $_{v}II_{i}$ from naïve control mice either with normal ACSF (top, "ACSF") or with ACSF containing bicuculline plus strychnine ("Bic+stry" group), Mrgprd-ablated mice ("*Mrgprd*^{CreERT2}-*DTR*" group), Mrgprd-ablation control mice with SNI ("*Mrgprd*^{CreERT2} or *DTR*&SNI" group), and Mrgprd-ablated mice with SNI (bottom, "*Mrgprd*^{CreERT2}-*DTR*&SNI"). Data for (A) are presented as mean ± SEM; Data for (B) are presented as percentage. "NS", no significance; **p < 0.01, ***p < 0.001, ****p < 0.0001. One-way ANOVA with holm-sidak test for (A); Chi-square test for (B). See also Figures S3 and S4.

neurons under neuropathic conditions. After SNI, 82% (18 of 22) of neurons had detectable C-eEPSCs, and 59% (13 of 22) of them fired AP which showed a dramatic increment compared with naïve control mice (Chi-square test, p < 0.0001) (Figure 4B). However, SNI-induced C-eAPs were reduced to 18% in Mrgprd-ablated mice (4 of 22; Chi-square test, p < 0.01) (Figure 4B). Correspondingly, the amplitude of C-eEPSCs was also reduced (Figure S3C). Thus, our data suggest that the opening of the gated C pathway in laminae $_{v}II_{i}$ is largely compromised when Mrgprd^{+} sensory neurons are ablated.

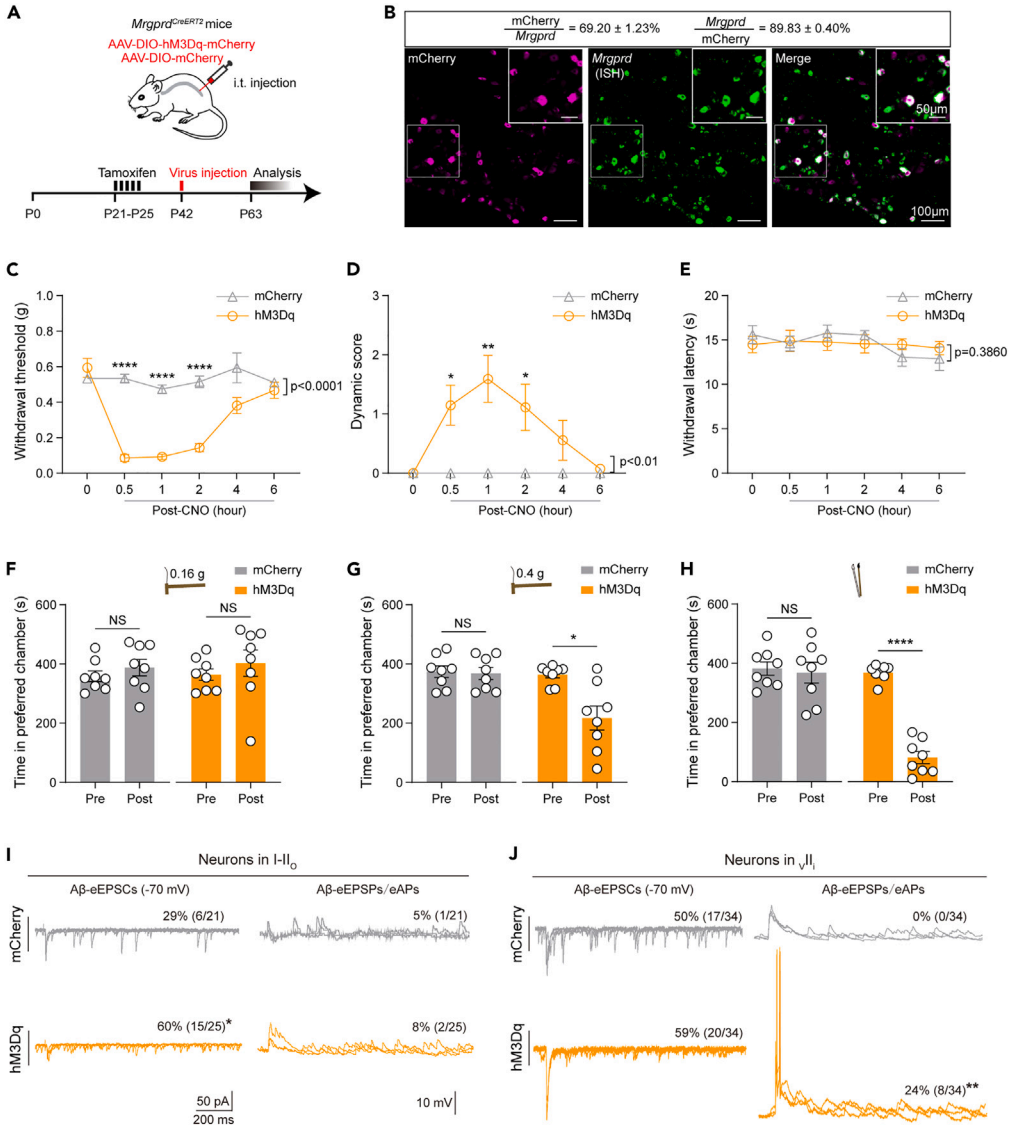

Figure 5. Chemogenetic activation of Mrgprd-expressing neurons drives mechanical allodynia and opens gated Aβ spinal pathway within γII$_i$

(A) An outline of the experimental scheme for tamoxifen treatment (i.p. 75 mg/kg tamoxifen per day, P21–P25), AAV treatment (i.t. 10 μL AAV-DIO-hM3Gq-mCherry, P42), and morphological or behavioral analysis (starting at P63) in *Mrgprd*^{CreERT2} mice.

(B) Co-localization of AAV-DIO-hM3Gq-mCherry (magenta) with *Mrgprd* mRNA (*ISH*, green) (bottom) and statistical data for overlap quantification (top) (69.20 ± 1.23% of Mrgprd$^+$ neurons co-express mCherry and 89.83 ± 0.40% of mCherry$^+$ cells that co-express *Mrgprd*) in lumbar DRG (n = 3 animals per group, 3 sections/animal). Scale bar 100 μm.

(C–E) Impact of Mrgprd$^+$ nociceptors activation on mechanical and thermal sensitivity. Mechanical hypersensitivity to von Frey filaments (C) and brush (D) developed while thermal sensitivity was unaffected (E) following i.p. injection of CNO (2 mg/kg) (n = 6 mice for mCherry group and n = 9 mice for hM3Dq group).

(F and G) Absolute time (s) spent in the preferred chamber before (pre) and after (post) conditioning by von Frey at 0.16 g (F) and 0.4 g (G) for mCherry and hM3Dq groups (n = 8 mice per group). RTPA test was carried out 20 min after CNO injection.

(H) Absolute time (s) spent in the preferred chamber before (pre) and after (post) conditioning by brush for mCherry and hM3Dq groups (n = 8 mice per group). RTPA test was carried out 20 min after CNO injection.

Figure 5. *Continued*

(I and J) Representative traces of Aβ-evoked inputs (left) and outputs (right) of the neurons in laminae I–II_o (I) and laminae $_vII_i$ (J) from mCherry (top) and hM3Dq (bottom) groups. Data for (B)–(H) are presented as mean ± SEM; Data for (I) and (J) are presented as percentage. "NS", no significance; *p < 0.05, **p < 0.01, ****p < 0.0001. Two-way repeated-measures ANOVA with holm-sidak test for (C)–(E); Paired Student's two-tailed t test or Wilcoxon signed-rank test for (F)–(H); Chi-square test for (I) and (J). See also Figures S5–S8 and S10.

Chemogenetic activation of Mrgprd-expressing neurons drives mechanical allodynia and opens gated Aβ spinal pathway within $_vII_i$ in intact mice

To further explore the role of $Mrgprd^+$ nociceptors in mechanical pain, we performed gain-of-function by using the chemogenetics with the excitatory hM3Dq designer receptor exclusively activated by designer drugs (DREADDs). After tamoxifen induction, adeno-associated virus (AAV) encoding Cre-dependent hM3Dq-mCherry or mCherry was intrathecally injected at P42 (Figure 5A). We found that ~69% of *Mrgprd* mRNA-containing DRG neurons expressed hM3Dq-mCherry (Figure 5B). Reciprocally, ~90% of hM3Dq-mCherry-positive neurons co-expressed *Mrgprd*, indicative of high specificity of viral targeting (Figure 5B). By performing whole-cell patch-clamp recordings on acutely dissociated hM3Dq-mCherry-positive DRG neurons, we discovered that clozapine-N-oxide (CNO) (10 μM) produced significant membrane depolarization (Figure S5), demonstrating the efficacy of the chemogenetic activation.

Following i.p. injection of CNO, hM3Dq-injected $Mrgprd^{CreERT2}$ mice manifested both von Frey-evoked punctate and brush-evoked dynamic hypersensitivity (Figures 5C and 5D). In contrast, thermal sensitivity was unchanged (Figure 5E). Thus, chemogenetic activation of $Mrgprd^+$ neurons preferentially enables low-threshold inputs to access nociceptive circuits to evoke behavioral responses.

To evaluate the affective aspects of static and dynamic allodynia arising from $Mrgprd^+$ nociceptors activation, RTPA assay was used again. After CNO treatment, we found low-threshold von Frey at 0.16 g evoked a transient aversion during the stimulation period (data not shown) while 0.4 g filament, as well as light brush, can provoke robust place aversion even after the simulation in hM3Dq-injected $Mrgprd^{CreERT2}$ mice (Figures 5F–5H). To validate these results, we also activated $Mrgprd^+$ sensory neurons by optogenetics. In $Mrgprd^{CreERT2}$; $ROSA^{ChR2\text{-}EYFP}$ mice (referred to as $Mrgprd^{CreERT2}$-*ChR2* mice) in which the non-peptidergic C-fiber subset was genetically labeled by ChR2 (Figures S6A–S6C), 10 min priming stimulation of hindpaw by blue light drove mechanical allodynia (Figures S6D–S6F). Following prolonged hindpaw transdermal blue light stimulation, $Mrgprd^{CreERT2}$-*ChR2* mice showed analogous aversion to 0.4 g filament and brush (Figures S6G–S6I).

We further examined the consequence of $Mrgprd^+$ neurons activation on the gated Aβ-fiber inputs pathway. By recording from superficial neurons (I–II_o), a significant increase of Aβ-eEPSCs, but not Aβ-eAPs, was observed: 60% (15 of 25) vs. 29% (6 of 21, Chi-square test, $p < 0.05$) in hM3Dq-injected $Mrgprd^{CreERT2}$ mice versus control mice (Figure 5I). Next, we examined Aβ inputs to neurons within $_vII_i$. The percentage of neurons displaying Aβ-eAPs was increased from 0% (0 of 34) to 24% (8 of 34, Chi-square test, $p < 0.01$) in control mice versus hM3Dq-injected $Mrgprd^{CreERT2}$ mice (Figure 5J). Chemogenetic activation produced-tonic APs in the $Mrgprd^+$ neurons may produce increases in EPSCs. We next recorded spontaneous EPSCs (sEPSCs) within $_vII_i$ neurons and found that the amplitude of sEPSCs was increased in hM3Dq-injected $Mrgprd^{CreERT2}$ mice compared with control mice (Figures S7A–S7C), suggesting postsynaptic glutamate receptor enhancement. Correspondingly, the amplitude of Aβ-eEPSCs was also increased (Figure S7D).

To further validate the above chemogenetics results, we performed another set of recordings after optogenetic activation (10 min) of hindpaw $Mrgprd^+$ fibers. By recording neurons in the superficial layer in which pain output neurons are mainly located, we observed an obvious trend of increment in the percentage of Aβ-eEPSCs and Aβ-eAPs: 27% (8 of 30) vs. 52% (11 of 21, Chi-square test, $p = 0.0616$), and 10% (3 of 30) vs. 29% (6 of 21, Chi-square test, $p = 0.0869$) in yellow light group versus blue light group, respectively (Figure S6J). Collectively, Mrgprd-expressing neural activation opens the gate for low-threshold mechanical afferents to the spinal dorsal horn.

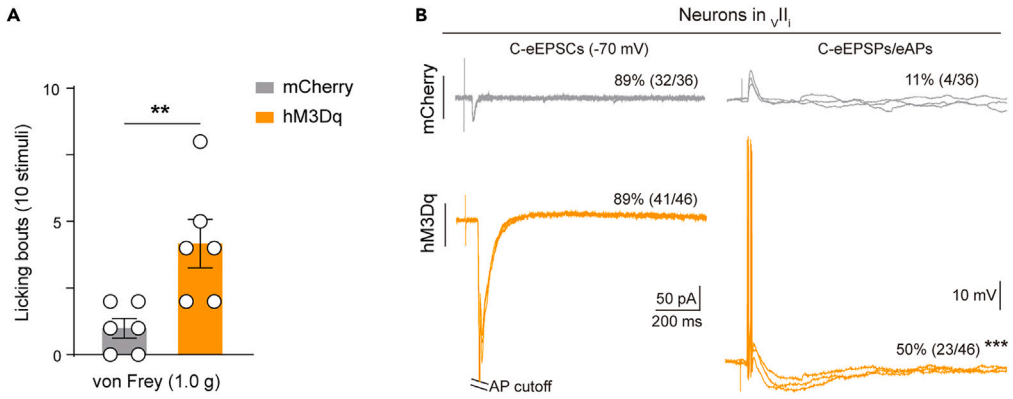

Figure 6. Sustained activation of Mrgprd-expressing neurons drives mechanical hyperalgesia and opens gated C inputs spinal pathway within ᵥIIᵢ

(A) Paw licking bouts in response to 10 trials of 1.0 g von Frey paw stimulation in mCherry-injected *Mrgprd*^{CreERT2} mice and hM3Dq-injected *Mrgprd*^{CreERT2} mice following i.p. injection of CNO (2 mg/kg) (n = 6 mice per group).

(B) Representative traces of C-evoked inputs (left) and outputs (right) of the neurons in laminae ᵥIIᵢ from mCherry (top) and hM3Dq (bottom) groups. Data for (A) are presented as mean ± SEM; Data for (B) are presented as percentage. **p < 0.01, ***p < 0.001. Unpaired Student's two-tailed t test for (A); Chi-square test for (B). See also Figures S7 and S8.

Chemogenetic activation of Mrgprd-expressing neurons drives mechanical hyperalgesia and opens gated C inputs spinal pathway within ᵥIIᵢ

To decipher the role of *Mrgprd*^{CreERT2}-marked neurons in mediating mechanical hyperalgesia, we applied high-threshold von Frey at 1.0 g. Following chemogenetic activation of Mrgprd-expressing neurons, 1.0 g von Frey filament drove more paw-licking behaviors which were rarely observed in control mice (Figure 6A), indicating the development of mechanical hyperalgesia. We then asked whether gated C-fiber inputs pathway within ᵥIIᵢ was opened by Mrgprd$^+$ nociceptors. We found that the percentage of neurons with C-eAPs increased from 11% (4 of 36) in control mice to 50% (23 of 46, Chi-square test, $p < 0.001$) in hM3Dq-injected *Mrgprd*^{CreERT2} mice (Figure 6B). Correspondingly, the amplitude of C-eEPSCs was enhanced (Figure S7E). Similarly, after optogenetic activation of hindpaw Mrgprd$^+$ fibers, we observed a significant increase of C-eEPSCs and C-eAPs: 74% (20 of 27) vs. 93% (28 of 30, Chi-square test, $p < 0.05$), and 11% (3 of 27) vs. 43% (13 of 30, Chi-square test, $p < 0.01$) in yellow light group versus blue light group, respectively (Figure S6K). From above, we postulate that the opened Aβ and C inputs pathway in laminae ᵥIIᵢ are the spinal substrates for mechanical allodynia and mechanical hyperalgesia, respectively.

Chemogenetic activation of Mrgprd-expressing neurons attenuates potassium currents within ᵥIIᵢ

Finally, we sought to investigate gate-opening mechanisms by Mrgprd$^+$ nociceptors. In the GCT, nociceptors inputs are proposed to reduce inhibitory neuron activity.[4] We therefore first assessed how Aβ-eIPSCs and C-eIPSCs within ᵥIIᵢ were affected in hM3Dq-injected *Mrgprd*^{CreERT2} mice. To our surprise, we detected comparable rates of ᵥIIᵢ neurons with Aβ-eIPSCs and C-eIPSCs between the two groups: 27% (9 of 33) vs. 23% (7 of 30, Chi-square test, $p = 0.720$), and 53% (20 of 38) vs. 58% (18 of 31, Chi-square test, $p = 0.652$) in hM3Dq-injected *Mrgprd*^{CreERT2} mice versus control mice, respectively (Figure 7A). To further investigate whether inhibitory synaptic efficacy was altered, we analyzed the amplitude of Aβ-eIPSCs and C-eIPSCs. They were also comparable between the two groups (Figures 7B and 7C). These results indicate that disinhibition may not be the major contributor.

We then hypothesized that chemogenetic activation of Mrgprd$^+$ neurons could sensitize the postsynaptic excitatory interneurons, making the gate control no longer work. To test this hypothesis, we first analyzed the resting membrane potentials (RMPs) of neurons in ᵥIIᵢ from control mice and hM3Dq-injected *Mrgprd*^{CreERT2} mice. However, similar RMPs were observed (mCherry: -56.8 ± 1.0 mV; hM3Dq: -55.9 ± 1.0 mV, two-tailed Student's unpaired test, $p = 0.524$) (Figure 7D). Therefore, the potassium leak channels, a major determinant of RMP, may be unaffected. In a previous study, we showed that prolonged TRPV1$^+$ nociceptors activation by capsaicin can open the gated Aβ pathway by attenuating the key neuronal firing

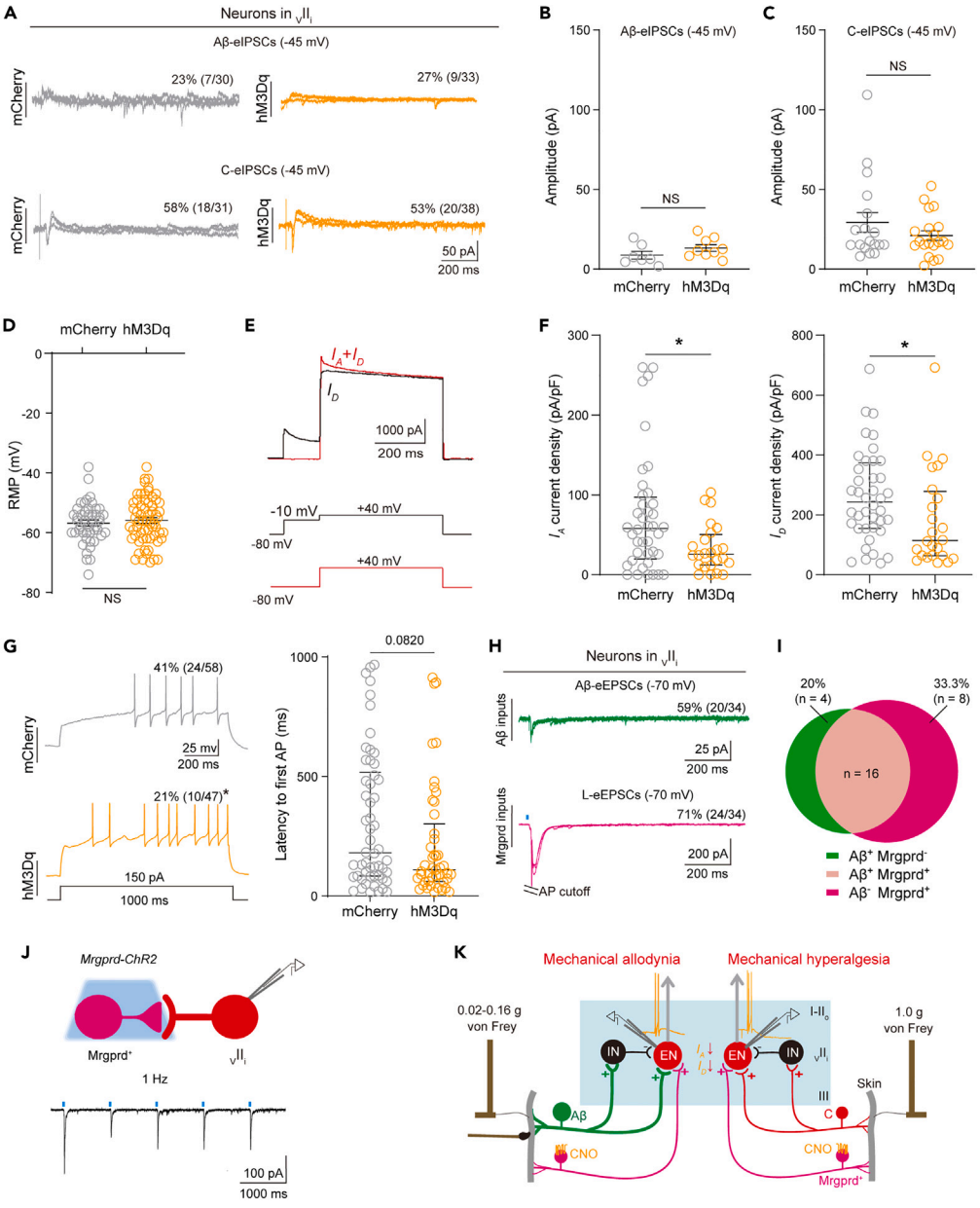

Figure 7. Chemogenetic activation of Mrgprd-expressing neurons attenuates potassium currents within ᵥIIi

(A) Representative traces of Aβ-eIPSCs (top) and C-eIPSCs (bottom) of the neurons in laminae ᵥIIi from mCherry-injected *Mrgprd*^{CreERT2} mice (left, "mCherry"), and hM3Dq-injected *Mrgprd*^{CreERT2} mice (right, "hM3Dq") following i.p. injection of CNO (2 mg/kg).

(B) Comparison of Aβ-eIPSCs amplitude of neurons in ᵥIIi between mCherry (n = 7 neurons) and hM3Dq (n = 9 neurons) groups.

(C) Comparison of C-eIPSCs amplitude of neurons in ᵥIIi between mCherry (n = 18 neurons) and hM3Dq (n = 20 neurons) groups.

(D) Comparison of resting membrane potentials (RMPs) of neurons within ᵥIIi between mCherry (n = 46 neurons) and hM3Dq (n = 62 neurons) groups.

(E) The two-step protocol for I_A recording. The first step was to record the total outward current (I_A + I_D) (red line). The second step was to record I_D by conditioning I_A inactivation. Subtraction of I_D from the total current isolated the I_A.

(F) Comparison of I_A (left) and I_D (right) current density of neurons in ᵥIIi between mCherry (n = 40 neurons for I_A and I_D current density) and hM3Dq (n = 24 neurons for I_A and I_D current density) groups.

(G) Comparison of percentage of delayed firing pattern (left) and AP firing latency (right) of neurons in ᵥIIi between mCherry (n = 54 neurons) and hM3Dq (n = 45 neurons) groups.

Figure 7. *Continued*

(H) Representative traces of Aβ-eEPSCs (top) and Mrgprd$^+$ inputs-evoked EPSCs (bottom) of the neurons in $_{v}II_i$ from *Mrgprd^{CreERT2}-ChR2* mice.

(I) Quantitative Venn diagram showing the percentage of neurons in $_{v}II_i$ that receive inputs from Mrgprd$^+$ neurons and/or Aβ-fibers.

(J) Schematic showing patch clamp recording in laminae $_{v}II_i$ neurons from *Mrgprd^{CreERT2}-ChR2* mice (top) and light-evoked EPSCs following 1 Hz light stimulation (bottom).

(K) Schematic showing the gate control mechanism of mechanical allodynia and hyperalgesia that subthreshold potassium channels plus a feedforward activation of inhibitory neurons ("IN") prevent Aβ and C inputs from activating excitatory neurons in $_{v}II_i$. The gated Aβ- and C-pathway within $_{v}II_i$ can be opened by chemogenetic activation of Mrgprd$^+$ nociceptors, partially via attenuating I_A and I_D rather than via disinhibition. Data for (A), (H), and (I) are presented as percentage; Data for (B), (C), and (D) are presented as mean ± SEM; Data for (F) and (G) are presented as median with interquartile range (Q1–Q3 with median denoted in between). "NS", no significance; *p < 0.05. Chi-square test for (A); Unpaired Student's two-tailed t test for (B), (D); Mann-Whitney *U* test for (C), (F), and (G). See also Figures S8 and S9.

threshold controller: A-type potassium currents (I_A).[36] We then examined whether I_A was affected by Mrgprd$^+$ nociceptors. To record I_A, a two-step voltage protocol was used (Figure 7E). After CNO treatment in hM3Dq-injected *Mrgprd^{CreERT2}* mice, I_A current density was remarkably reduced compared with control mice (mCherry: median, 58 pA/pF; Q1–Q3: 20–97 pA/pF; hM3Dq: median, 26 pA/pF; Q1–Q3, 12–51 pA/pF; Mann-Whitney *U* Test, p < 0.05) (Figure 7F, **left**). Accordingly, the neurons with delayed firing, an indication of strong I_A, decreased from 41% (24 of 58) to 21% (10 of 47, Chi-square test, p < 0.05) (Figure 7G, **left**), and the latency to AP firing following current injection tended to be shortened (mCherry: median, 180.6 ms; Q1–Q3: 83.05–517 ms; hM3Dq: median, 110.0 ms; Q1–Q3, 60.65–300.9 ms; Mann-Whitney *U* Test, p = 0.082) (Figure 7G, right). Meanwhile, the current density of persistent potassium channel activity (I_D) was also attenuated (mCherry: median, 244 pA/pF; Q1–Q3: 155–374 pA/pF; hM3Dq: median, 114 pA/pF; Q1–Q3, 64–278 pA/pF; Mann-Whitney *U* Test, p < 0.05) (Figure 7F, **right**).

What are the identities of neurons within $_{v}II_i$ sensitized by Mrgprd$^+$ nociceptors? Earlier tracing studies showed that few neurons in $_{v}II_i$ containing ascending projections, thereby reflecting interneurons.[37] Given that inhibitory neurons account for ~25% of the total neuronal population in laminae I–II,[38] the neurons we recorded above could be a mixture of both excitatory (by a large chance) and inhibitory interneurons. We next specifically assessed the excitatory neurons with VGLUT2 promoter-driven viral labeling (Figures S8A and S8B) and found that the percentage of VGLUT2$^+$ neurons in $_{v}II_i$ with Aβ-eAPs increased by 15%, from 0 (0 of 24) in controls to 15% (4 of 26) in hM3Dq-injected *Mrgprd^{CreERT2}* mice, and C-APs increased by 35% from 13% (3 of 24) in controls to 48% (10 of 21) in hM3Dq-injected *Mrgprd^{CreERT2}* mice (Figure S8C). Thus, Mrgprd$^+$ nociceptors-sensitized neurons within $_{v}II_i$ are predominantly VGLUT2-positive neurons. Correspondingly, the amplitude of Aβ-eEPSCs and C-eEPSCs was enhanced (Figures S8D and S8E). Consistent with previous recordings from randomly picked neurons, RMP was comparable between the two groups (Figure S8F). The membrane resistance was also similar (Figure S8G), further supporting that the potassium leak channels were unaffected. As postulated, both I_A and I_D current density of VGLUT2-positive excitatory neurons in $_{v}II_i$ were remarkably attenuated (Figures S8H and S8I).

In dorsal horn neurons, the Kv4.2 potassium channel contributes to I_A,[39] and activation of extracellular-signal-regulated kinases (ERKs) reduces Kv4.2 activity via phosphorylation.[40] Strong nociceptor inputs (like capsaicin injection)-induced mechanical allodynia can be occluded by blocking MEK-pERK signaling which mediates I_A reduction.[36] We proposed that Mrgprd$^+$ nociceptors might act through the similar mechanism to cause mechanical allodynia. To test this, we examined whether static and dynamic allodynia after Mrgprd$^+$ neurons activation was abolished by MEK kinase inhibitor PD98059. As expected, intrathecal injection of PD98059 prevented the development of both static and dynamic allodynia (Figure S9), indicating an indispensable role of MEK-pERK signaling in Mrgprd$^+$-recruited gate-opening of mechanical hypersensitivity.

To further clarify the influence of Mrgprd$^+$ nociceptors activation on Aβ inputs spinal pathway, we next recorded blue light-evoked EPSCs (L-eEPSCs) and Aβ-eEPSCs of neurons within $_{v}II_i$ simultaneously in naïve *Mrgprd^{CreERT2}-ChR2* mice. First of all, we detected 59% (20 of 34) and 71% (24 of 34) of neurons in the $_{v}II_i$ receiving Aβ and Mrgprd$^+$ inputs, respectively (Figure 7H). Interestingly, we observed that the majority (16 of 20, 80%) of recorded neurons with Aβ-EPSCs received L-eEPSCs (Figure 7I). Furthermore, 30% (6 of 20) of neurons with L-eEPSCs showed no failure following 1 Hz light stimulation and

showed low-response jitter (variability in latency: 0.97 ± 0.36 ms), indicative monosynaptic connections with Mrgprd$^+$ afferents[41] (Figure 7J). Reciprocally, 67% (16 of 24) of neurons with L-EPSCs received Aβ-eEPSCs. Surprisingly, 100% (6 of 6) of neurons that receive monosynaptic input from Mrgprd$^+$ afferents also receive Aβ inputs. We inferred that most neurons within $_{v}II_{i}$ receive convergent inputs from Mrgprd$^+$ nociceptors (directly or indirectly) and Aβ fibers, which supports us to propose the sensitization mode: activation of Mrgprd$^+$ nociceptors attenuates potassium channel activity of the neurons receiving convergent Aβ and Mrgprd$^+$ inputs, resulting in gate-opening of Aβ inputs spinal pathways and mechanical allodynia (Figure 7K, **left**). Collectively, Mrgprd$^+$ nociceptors drive mechanical allodynia and hyperalgesia, and open gated Aβ and C inputs spinal pathways, partially via attenuating potassium channel activity rather than disinhibition (Figure 7K).

DISCUSSION

Taking advantage of an inducible *Mrgprd^{CreERT2}* mouse line that allows for temporally controlled genetic manipulation, we studied the role of adult Mrgprd$^+$ neurons in nerve injury-induced mechanical pain and deciphered the underlying spinal substrates, which provided potential targets for effective pain management.

First, we verified the high efficiency and specificity of adult Mrgprd-expressing DRG neurons ablation, without loss of peptidergic C-fiber neurons labeled by CGRP, C-LTMRs neurons labeled by TH, and myelinated Aβ/Aδ-fiber neurons labeled by NF-200 (Figure S1). The percentage of functional Aβ/C inputs to the spinal dorsal horn was also unaltered (Figures 3B, 3C, and 4). Behaviorally, after nerve injury, we observed a selective attenuation of von Frey-induced static allodynia and aversion, without a deficit of brush-induced dynamic allodynia (Figures 1 and 2). Paw withdrawal induced by innocuous stimuli is mainly mediated by LTMRs (like Aβ-LTMR) after SNI.[42,43] Consistently, the withdrawal threshold was reduced to ~0.02 g, and such thresholds reflect the involvement of LTMRs since activation thresholds of nociceptors (such as Mrgprd$^+$) were around 0.5–5 g.[7,44] The fact that in Mrgprd-ablated mice, the SNI-induced withdrawal threshold was raised up to ~0.3 g suggests two insights. Firstly, LTMRs apparently fail to drive sensitized reflexes (with thresholds at ~0.02 g in wild-type mice with SNI). The attenuated static allodynia is supported by our electrophysiological recordings, showing a marked loss of Aβ stimulation-evoked AP firing in lamina $_{v}II_{i}$ (Figure 3C), a region receiving convergent inputs from Aβ fibers and Mrgprd$^+$ C-fibers. Secondly, Mrgprd-negative nociceptors, which normally drive reflexes at the threshold of ~1.3 g in Mrgprd-ablated mice without SNI, can be sensitized to produce reflexes at the threshold of ~0.3 g, and future studies will be warranted to characterize such nociceptors, such as recently reported silent nociceptors that can gain mechanical sensitivity under pathological conditions.[45] The remaining 33% of Aβ inputs to laminae I–II_{o} preserved in Mrgprd-ablated mice might sufficiently serve as the neural substrate for dynamic allodynia that is preserved in Mrgprd-ablated mice. Of note, this is different from gain-of-function studies, where central sensitization induced by Mrgprd$^+$ neuronal activation can sufficiently drive dynamic allodynia. In other words, while gain-of-function studies may reveal redundant pathways, loss-of-function studies may fail to reveal such redundancy. Furthermore, we also ablated these neurons in established neuropathic pain mice to assess whether Mrgprd$^+$ fibers are required for the maintenance of mechanical allodynia after nerve injury. The SNI-induced withdrawal threshold was raised up to >0.3 g (Figure 1). Overall, our study may advance the current understanding of Mrgprd$^+$ neurons in both the development and maintenance of neuropathic pain.

In humans, two forms of short-lasting pain can develop following noxious stimulation: first pain with a sharp, pricking, stinging, and precisely localized quality[46] and delayed second pain with a burning, dull, and diffuse quality.[47,48] They are possibly mediated by fast-conducting thinly myelinated Aδ nociceptors and slow-conducting unmyelinated C nociceptors,[34,46] respectively. In naïve control mice, high-threshold von Frey (1.0 g) produced mostly paw-lifting behaviors. After SNI, when 1.0 g von Frey filament was applied to the hindpaw plantar, we observed both fast-onset paw lifting and delayed paw fluttering (Figure 4A), indicative of mechanical hyperalgesia.[32,33] Intriguingly, such paw fluttering response was dramatically reduced in Mrgprd-ablated mice (Figure 4A), in which the opening of C-gate after nerve injury was largely abolished (Figure 4B). These results suggested that the observed paw fluttering might be a manifestation of second pain in humans which can be self-reported. Mechanistically, the opened "C-gate" after nerve injury could transmit delayed second pain, much like capsaicin-sensitive mechanonociceptors-mediated second pain in humans.[34]

To further investigate how Mrgprd$^+$ nociceptors affect low-threshold and high-threshold von Frey filaments-evoked responses and gated Aβ/C inputs, we performed the gain-of-function experiments. We demonstrated that the amplitude of sEPSCs was increased after chemogenetic activation of Mrgprd$^+$ neurons (Figure S7B). However, the enhanced sEPSC itself was insufficient to evoke spontaneous AP within $_{v}II_{i}$ neurons, while activation of Mrgprd$^+$ neurons facilitated the gated Aβ/C inputs opening (Figures 5J and 6B). By using optogenetic temporally-specific activation, we acquired similar results that Mrgprd$^+$ neural activation opens the gate for Aβ/C inputs to the spinal dorsal horn (Figures S6J and S6K).

We next explored the gate-opening mechanisms following Mrgprd$^+$ neurons activation. We found that $_{v}II_{i}$ neurons that receive monosynaptic inputs from Mrgprd$^+$ neurons also receive convergent inputs from Aβ fibers, and these neurons are sensitized following Mrgprd$^+$ neurons activation partially via inactivation of I_A currents (Figure 7), which are involved in the electric filtering of synaptic responses[49,50] and behaviorally gate mechanical pain.[36,39,51] To further illustrate the role of I_A currents-mediated sensitization in mechanical allodynia following Mrgprd$^+$ neurons activation, we examined the necessity of ERK-dependent potassium currents modulation, which is perceived as a key mechanism for the central sensitization in the development of allodynia,[39,52–54] and revealed an indispensable role of MEK-pERK signaling in Mrgprd$^+$-recruited gate-opening of mechanical hypersensitivity (Figure S9). Our ideas on central sensitization are also supported by prominent pain investigator Clifford J. Woolf's description "central sensitization represented a condition where input in one set of nociceptor sensory fibers (the conditioning input) amplified subsequent responses to other non-stimulated non-nociceptor or nociceptor fibers."[52] Combined with our recording data on VGLUT2$^+$ neurons (Figure S8) and a recent study showing SNI selectively decreases I_A in spinal excitatory interneurons,[55] we propose that SNI possibly activates Mrgprd$^+$ neurons in a persistent manner, leading to central sensitization of excitatory neurons within $_{v}II_{i}$ receiving convergent inputs from Mrgprd$^+$ nociceptors and Aβ fibers, which allows Aβ inputs to open the gate for mechanical allodynia. Future study is needed to assess the molecular identity of the excitatory neurons recruited by Mrgprd$^+$ nociceptors to convey mechanical allodynia. For example, somatostatin-expressing spinal interneurons, which were synaptically connected with Mrgprd$^+$ neurons[56] and necessary for TRPV1$^+$ nociceptors activation-induced mechanical allodynia, may be involved.[36]

The mechanical allodynia and real-time operant escape assays in response to low-threshold mechanical force, as well as paw fluttering/licking in response to high-threshold von Frey filament after nerve injury or Mrgprd$^+$ neurons activation, by nature, represent short-lasting phasic pain and exteroceptive.[57] What's the role of Mrgprd$^+$ neurons in clinically more relevant tonic pain under chronic neuropathic conditions? Previous studies showed that *Runx1*-transient TRPV1$^{low\text{-}medium}$ chemosensitive neurons rather than *Runx1*-persistent Mrgprd$^+$ neurons were indispensable for inescapable pinch-evoked licking responses and aversive experience under normal conditions.[45,57,58] Our recent study[19] and preliminary data showed that optogenetic or chemogenetic activation of Mrgprd$^+$ neurons can drive spontaneous licking response and conditioned place avoidance (CPA) after SNI which were absent in naïve conditions (Figure S10). These results indicate that Mrgprd$^+$ neurons might be involved in tonic pain and interoceptive self-caring behaviors under neuropathic conditions. Future loss-of-function experiments are needed to test this possibility. Nevertheless, our study provides mechanistic insights into the development of neuropathic pain. The existence of distinct mechanisms driving distinct forms of neuropathic pain suggests the necessity of developing a cocktail of drugs for blocking distinct pain pathways.

Limitations of the study

Although our study showed that activation of Mrgprd$^+$ neurons evoked central sensitization by attenuation of K$^+$ current, future studies need to address which type of neurotransmitter or peptides from Mrgprd$^+$ DRG neurons are involved in the central sensitization to drive allodynia. In addition, the identity of neurons that received convergent inputs from Mrgprd$^+$ neurons and Aβ fibers is still unclear.

STAR★METHODS

Detailed methods are provided in the online version of this paper and include the following:

- KEY RESOURCES TABLE
- RESOURCE AVAILABILITY
  - Lead contact
  - Materials availability

SUPPLEMENTAL INFORMATION

Supplemental information can be found online at https://doi.org/10.1016/j.isci.2023.106764.

ACKNOWLEDGMENTS

We thank Dr. Yuanyuan Liu in NIH for critical comments and editing on the manuscript. We also thank Dr. Tianwen Huang in Shenzhen Institute of Advanced Technology for the technical advice on *in situ* hybridization. This study was supported by the National Natural Science Foundation of China (32070999, 32271048, and U20A20357), Anhui Provincial Natural Science Foundation (grant 2008085J16), and the Fundamental Research Funds for the Central Universities (WK2070210004 and WK9110000056).

AUTHOR CONTRIBUTIONS

Y.Z. and L.B.W. designed the project. X.J.S., J.J.Y., and Y.Z. generated electrophysiology data and contributed to their analysis. L.B.W., X.J.S., and W.H. performed all the behavioral and immunofluorescence experiments. L.B.W. and Q.F.W. conducted *in situ* hybridization. X.X. and X.Q.L. managed the mouse colonies used in this study. X.Y.W. performed nerve injury model. X.F.L. and Y.Z. supervised the project. Y.Z. and L.B.W. wrote the first draft. All authors reviewed and edited the draft.

DECLARATION OF INTERESTS

The authors declare no competing interests.

Received: August 23, 2022
Revised: March 17, 2023
Accepted: April 24, 2023
Published: April 27, 2023

REFERENCES

1. Costigan, M., Scholz, J., and Woolf, C.J. (2009). Neuropathic pain: a maladaptive response of the nervous system to damage. Annu. Rev. Neurosci. *32*, 1–32. https://doi.org/10.1146/annurev.neuro.051508.135531.

2. Jensen, T.S., and Finnerup, N.B. (2014). Allodynia and hyperalgesia in neuropathic pain: clinical manifestations and mechanisms. Lancet Neurol. *13*, 924–935. https://doi.org/10.1016/S1474-4422(14)70102-4.

3. Benyamin, R., Trescot, A.M., Datta, S., Buenaventura, R., Adlaka, R., Sehgal, N., Glaser, S.E., and Vallejo, R. (2008). Opioid complications and side effects. Pain Physician *11*, S105–S120. https://doi.org/10.36076/ppj.2008/11/s105.

4. Melzack, R., and Wall, P.D. (1965). Pain mechanisms: a new theory. Science *150*, 971–979. https://doi.org/10.1126/science.150.3699.971.

5. Latremoliere, A., and Woolf, C.J. (2009). Central sensitization: a generator of pain hypersensitivity by central neural plasticity. J. Pain *10*, 895–926. https://doi.org/10.1016/j.jpain.2009.06.012.

6. Prescott, S.A. (2015). Synaptic inhibition and disinhibition in the spinal dorsal horn. Prog. Mol. Biol. Transl. Sci. *131*, 359–383. https://doi.org/10.1016/bs.pmbts.2014.11.008.

7. Rau, K.K., McIlwrath, S.L., Wang, H., Lawson, J.J., Jankowski, M.P., Zylka, M.J., Anderson, D.J., and Koerber, H.R. (2009). Mrgprd enhances excitability in specific populations of cutaneous murine polymodal nociceptors. J. Neurosci. *29*, 8612–8619. https://doi.org/10.1523/JNEUROSCI.1057-09.2009.

8. Yang, F.-C., Tan, T., Huang, T., Christianson, J., Samad, O.A., Liu, Y., Roberson, D., Davis, B.M., and Ma, Q. (2013). Genetic control of the segregation of pain-related sensory neurons innervating the cutaneous versus deep tissues. Cell Rep. *5*, 1353–1364. https://doi.org/10.1016/j.celrep.2013.11.005.

9. Zylka, M.J., Rice, F.L., and Anderson, D.J. (2005). Topographically distinct epidermal nociceptive circuits revealed by axonal tracers targeted to Mrgprd. Neuron *45*, 17–25. https://doi.org/10.1016/j.neuron.2004.12.015.

10. Lou, S., Pan, X., Huang, T., Duan, B., Yang, F.-C., Yang, J., Xiong, M., Liu, Y., and Ma, Q. (2015). Incoherent feed-forward regulatory loops control segregation of C-mechanoreceptors, nociceptors, and pruriceptors. J. Neurosci. *35*, 5317–5329. https://doi.org/10.1523/JNEUROSCI.0122-15.2015.

11. Olson, W., Abdus-Saboor, I., Cui, L., Burdge, J., Raabe, T., Ma, M., and Luo, W. (2017). Sparse genetic tracing reveals regionally specific functional organization of mammalian nociceptors. Elife *6*, e29507. https://doi.org/10.7554/eLife.29507.

12. Warwick, C., Cassidy, C., Hachisuka, J., Wright, M.C., Baumbauer, K.M., Adelman, P.C., Lee, K.H., Smith, K.M., Sheahan, T.D., Ross, S.E., and Koerber, H.R. (2021). MrgprdCre lineage neurons mediate optogenetic allodynia through an emergent polysynaptic circuit. Pain *162*, 2120–2131. https://doi.org/10.1097/j.pain.0000000000002227.

13. Abrahamsen, B., Zhao, J., Asante, C.O., Cendan, C.M., Marsh, S., Martinez-Barbera, J.P., Nassar, M.A., Dickenson, A.H., and Wood, J.N. (2008). The cell and molecular basis of mechanical, cold, and inflammatory pain. Science *321*, 702–705. https://doi.org/10.1126/science.1156916.

14. Cavanaugh, D.J., Lee, H., Lo, L., Shields, S.D., Zylka, M.J., Basbaum, A.I., and Anderson, D.J. (2009). Distinct subsets of unmyelinated primary sensory fibers mediate behavioral responses to noxious thermal and mechanical stimuli. Proc. Natl. Acad. Sci. USA *106*, 9075–9080. https://doi.org/10.1073/pnas.0901507106.

15. Lan, L., Xu, M., Li, J., Liu, L., Xu, M., Zhou, C., Shen, L., Tang, Z., and Wan, F. (2020). Mas-related G protein-coupled receptor D participates in inflammatory pain by promoting NF-κB activation through interaction with TAK1 and IKK complex. Cell. Signal. *76*, 109813. https://doi.org/10.1016/j.cellsig.2020.109813.

16. Wang, C., Gu, L., Ruan, Y., Geng, X., Xu, M., Yang, N., Yu, L., Jiang, Y., Zhu, C., Yang, Y., et al. (2019). Facilitation of MrgprD by TRP-A1 promotes neuropathic pain. Faseb. J. *33*, 1360–1373. https://doi.org/10.1096/fj.201800615RR.

17. Beaudry, H., Daou, I., Ase, A.R., Ribeiro-da-Silva, A., and Séguéla, P. (2017). Distinct behavioral responses evoked by selective optogenetic stimulation of the major TRPV1+ and MrgD+ subsets of C-fibers. Pain *158*, 2329–2339. https://doi.org/10.1097/j.pain.0000000000001016.

18. Sharif, B., Ase, A.R., Ribeiro-da-Silva, A., and Séguéla, P. (2020). Differential coding of itch and pain by a subpopulation of primary afferent neurons. Neuron *106*, 940–951.e4. https://doi.org/10.1016/j.neuron.2020.03.021.

19. Wang, L.-B., Su, X.-J., Wu, Q.-F., Xu, X., Wang, X.-Y., Chen, M., Ye, J.-R., Maimaitiabula, A., Liu, X.-Q., Sun, W., and Zhang, Y. (2022). Parallel spinal pathways for transmitting reflexive and affective dimensions of nocifensive behaviors evoked by selective activation of the mas-related G protein-coupled receptor D-positive and transient receptor potential vanilloid 1-positive subsets of nociceptors. Front. Cell. Neurosci. *16*, 910670. https://doi.org/10.3389/fncel.2022.910670.

20. Ferrini, F., Perez-Sanchez, J., Ferland, S., Lorenzo, L.-E., Godin, A.G., Plasencia-Fernandez, I., Cottet, M., Castonguay, A., Wang, F., Salio, C., et al. (2020). Differential chloride homeostasis in the spinal dorsal horn locally shapes synaptic metaplasticity and modality-specific sensitization. Nat. Commun. *11*, 3935. https://doi.org/10.1038/s41467-020-17824-y.

21. Decosterd, I., and Woolf, C.J. (2000). Spared nerve injury: an animal model of persistent peripheral neuropathic pain. Pain *87*, 149–158. https://doi.org/10.1016/S0304-3959(00)00276-1.

22. Chamessian, A., Matsuda, M., Young, M., Wang, M., Zhang, Z.-J., Liu, D., Tobin, B., Xu, Z.-Z., Van de Ven, T., and Ji, R.-R. (2019). Is optogenetic activation of Vglut1-positive Aβ low-threshold mechanoreceptors sufficient to induce tactile allodynia in mice after nerve injury? J. Neurosci. *39*, 6202–6215. https://doi.org/10.1523/JNEUROSCI.2064-18.2019.

23. Porreca, F., and Navratilova, E. (2017). Reward, motivation, and emotion of pain and its relief. Pain *158*, S43–S49. https://doi.org/10.1097/j.pain.0000000000000798.

24. Rodriguez, E., Sakurai, K., Xu, J., Chen, Y., Toda, K., Zhao, S., Han, B.-X., Ryu, D., Yin, H., Liedtke, W., and Wang, F. (2017). A craniofacial-specific monosynaptic circuit enables heightened affective pain. Nat. Neurosci. *20*, 1734–1743. https://doi.org/10.1038/s41593-017-0012-1.

25. Koltzenburg, M., Lundberg, L.E.R., and Torebjörk, E.H. (1992). Dynamic and static components of mechanical hyperalgesia in human hairy skin. Pain *51*, 207–219. https://doi.org/10.1016/0304-3959(92)90262-A.

26. Ochoa, J.L., and Yarnitsky, D. (1993). Mechanical hyperalgesias in neuropathic pain patients: dynamic and static subtypes. Ann. Neurol. *33*, 465–472. https://doi.org/10.1002/ana.410330509.

27. Torebjörk, H.E., Lundberg, L.E., and LaMotte, R.H. (1992). Central changes in processing of mechanoreceptive input in capsaicin-induced secondary hyperalgesia in humans. J. Physiol. *448*, 765–780. https://doi.org/10.1113/jphysiol.1992.sp019069.

28. Cheng, L., Duan, B., Huang, T., Zhang, Y., Chen, Y., Britz, O., Garcia-Campmany, L., Ren, X., Vong, L., Lowell, B.B., et al. (2017). Identification of spinal circuits involved in touch-evoked dynamic mechanical pain. Nat. Neurosci. *20*, 804–814. https://doi.org/10.1038/nn.4549.

29. Duan, B., Cheng, L., Bourane, S., Britz, O., Padilla, C., Garcia-Campmany, L., Krashes, M., Knowlton, W., Velasquez, T., Ren, X., et al. (2014). Identification of spinal circuits transmitting and gating mechanical pain. Cell *159*, 1417–1432. https://doi.org/10.1016/j.cell.2014.11.003.

30. Lu, Y., Dong, H., Gao, Y., Gong, Y., Ren, Y., Gu, N., Zhou, S., Xia, N., Sun, Y.-Y., Ji, R.-R., and Xiong, L. (2013). A feed-forward spinal cord glycinergic neural circuit gates mechanical allodynia. J. Clin. Invest. *123*, 4050–4062. https://doi.org/10.1172/JCI70026.

31. Wercberger, R., and Basbaum, A.I. (2019). Spinal cord projection neurons: a superficial, and also deep analysis. Curr. Opin. Physiol. *11*, 109–115. https://doi.org/10.1016/j.cophys.2019.10.002.

32. Garrison, S.R., Weyer, A.D., Barabas, M.E., Beutler, B.A., and Stucky, C.L. (2014). A gain-of-function voltage-gated sodium channel 1.8 mutation drives intense hyperexcitability of A- and C-fiber neurons. PAIN® *155*, 896–905. https://doi.org/10.1016/j.pain.2014.01.012.

33. Hogan, Q., Sapunar, D., Modric-Jednacak, K., and McCallum, J.B. (2004). Detection of neuropathic pain in a rat model of peripheral nerve injury. Anesthesiology *101*, 476–487. https://doi.org/10.1097/00000542-200408000-00030.

34. Magerl, W., Fuchs, P.N., Meyer, R.A., and Treede, R.-D. (2001). Roles of capsaicin-insensitive nociceptors in cutaneous pain and secondary hyperalgesia. Brain *124*, 1754–1764. https://doi.org/10.1093/brain/124.9.1754.

35. Abraira, V.E., and Ginty, D.D. (2013). The sensory neurons of touch. Neuron *79*, 618–639. https://doi.org/10.1016/j.neuron.2013.07.051.

36. Zhang, Y., Liu, S., Zhang, Y.-Q., Goulding, M., Wang, Y.-Q., and Ma, Q. (2018). Timing mechanisms underlying gate control by feedforward inhibition. Neuron *99*, 941–955.e4. https://doi.org/10.1016/j.neuron.2018.07.026.

37. Hylden, J.L., Anton, F., and Nahin, R.L. (1989). Spinal lamina I projection neurons in the rat: collateral innervation of parabrachial area and thalamus. Neuroscience *28*, 27–37.

https://doi.org/10.1016/0306-4522(89)90229-7.

38. Polgár, E., Durrieux, C., Hughes, D.I., and Todd, A.J. (2013). A quantitative study of inhibitory interneurons in laminae I-III of the mouse spinal dorsal horn. PLoS One *8*, e78309. https://doi.org/10.1371/journal.pone.0078309.

39. Hu, H.-J., Carrasquillo, Y., Karim, F., Jung, W.E., Nerbonne, J.M., Schwarz, T.L., and Gereau, R.W. (2006). The Kv4.2 potassium channel subunit is required for pain plasticity. Neuron *50*, 89–100. https://doi.org/10.1016/j.neuron.2006.03.010.

40. Hu, H.-J., Alter, B.J., Carrasquillo, Y., Qiu, C.-S., and Gereau, R.W. (2007). Metabotropic glutamate receptor 5 modulates nociceptive plasticity via extracellular signal-regulated kinase–Kv4.2 signaling in spinal cord dorsal horn neurons. J. Neurosci. *27*, 13181–13191. https://doi.org/10.1523/JNEUROSCI.0269-07.2007.

41. Wang, H., and Zylka, M.J. (2009). Mrgprd-expressing polymodal nociceptive neurons innervate most known classes of substantia gelatinosa neurons. J. Neurosci. *29*, 13202–13209. https://doi.org/10.1523/JNEUROSCI.3248-09.2009.

42. La, J.-H., and Chung, J.M. (2017). Peripheral afferents and spinal inhibitory system in dynamic and static mechanical allodynia. Pain *158*, 2285–2289. https://doi.org/10.1097/j.pain.0000000000001055.

43. Seal, R.P., Wang, X., Guan, Y., Raja, S.N., Woodbury, C.J., Basbaum, A.I., and Edwards, R.H. (2009). Injury-induced mechanical hypersensitivity requires C-low threshold mechanoreceptors. Nature *462*, 651–655. https://doi.org/10.1038/nature08505.

44. Baumbauer, K.M., DeBerry, J.J., Adelman, P.C., Miller, R.H., Hachisuka, J., Lee, K.H., Ross, S.E., Koerber, H.R., Davis, B.M., and Albers, K.M. (2015). Keratinocytes can modulate and directly initiate nociceptive responses. Elife *4*, e09674. https://doi.org/10.7554/eLife.09674.

45. Prato, V., Taberner, F.J., Hockley, J.R.F., Callejo, G., Arcourt, A., Tazir, B., Hammer, L., Schad, P., Heppenstall, P.A., Smith, E.S., and Lechner, S.G. (2017). Functional and molecular characterization of mechanoinsensitive "silent" nociceptors. Cell Rep. *21*, 3102–3115. https://doi.org/10.1016/j.celrep.2017.11.066.

46. Handwerker, H.O., and Kobal, G. (1993). Psychophysiology of experimentally induced pain. Physiol. Rev. *73*, 639–671. https://doi.org/10.1152/physrev.1993.73.3.639.

47. Head, H., Rivers, W.H.R., and Sherren, J. (1905). The afferent nervous system from a new aspect. Brain *28*, 99–115. https://doi.org/10.1093/brain/28.2.99.

48. Lewis, T., and Pochin, E.E. (1937). The double pain response of the human skin to a single stimulus. Clin. Sci. *3*, 67–76.

49. Harnett, M.T., Xu, N.-L., Magee, J.C., and Williams, S.R. (2013). Potassium channels control the interaction between active dendritic integration compartments in layer 5 cortical pyramidal neurons. Neuron *79*, 516–529. https://doi.org/10.1016/j.neuron.2013.06.005.

50. Hoffman, D.A., Magee, J.C., Colbert, C.M., and Johnston, D. (1997). K+ channel regulation of signal propagation in dendrites of hippocampal pyramidal neurons. Nature *387*, 869–875. https://doi.org/10.1038/43119.

51. Clerc, N., and Moqrich, A. (2022). Diverse roles and modulations of IA in spinal cord pain circuits. Cell Rep. *38*, 110588. https://doi.org/10.1016/j.celrep.2022.110588.

52. Woolf, C.J. (2011). Central sensitization: implications for the diagnosis and treatment of pain. Pain *152*, S2–S15. https://doi.org/10.1016/j.pain.2010.09.030.

53. Ji, R.-R., Baba, H., Brenner, G.J., and Woolf, C.J. (1999). Nociceptive-specific activation of ERK in spinal neurons contributes to pain hypersensitivity. Nat. Neurosci. *2*, 1114–1119. https://doi.org/10.1038/16040.

54. Ji, R.-R., Kohno, T., Moore, K.A., and Woolf, C.J. (2003). Central sensitization and LTP: do pain and memory share similar mechanisms? Trends Neurosci. *26*, 696–705. https://doi.org/10.1016/j.tins.2003.09.017.

55. Yoo, S., Santos, C., Reynders, A., Marics, I., Malapert, P., Gaillard, S., Charron, A., Ugolini, S., Rossignol, R., El Khallouqi, A., et al. (2021). TAFA4 relieves injury-induced mechanical hypersensitivity through LDL receptors and modulation of spinal A-type K+ current. Cell Rep. *37*, 109884. https://doi.org/10.1016/j.celrep.2021.109884.

56. Wang, H., Chen, W., Dong, Z., Xing, G., Cui, W., Yao, L., Zou, W.-J., Robinson, H.L., Bian, Y., Liu, Z., et al. (2022). A novel spinal neuron connection for heat sensation. Neuron *110*, 2315–2333.e6. https://doi.org/10.1016/j.neuron.2022.04.021.

57. Ma, Q. (2022). A functional subdivision within the somatosensory system and its implications for pain research. Neuron *110*, 749–769. https://doi.org/10.1016/j.neuron.2021.12.015.

58. Huang, T., Lin, S.-H., Malewicz, N.M., Zhang, Y., Zhang, Y., Goulding, M., LaMotte, R.H., and Ma, Q. (2019). Identifying the pathways required for coping behaviours associated with sustained pain. Nature *565*, 86–90. https://doi.org/10.1038/s41586-018-0793-8.

59. Chaplan, S.R., Bach, F.W., Pogrel, J.W., Chung, J.M., and Yaksh, T.L. (1994). Quantitative assessment of tactile allodynia in the rat paw. J. Neurosci. Methods *53*, 55–63. https://doi.org/10.1016/0165-0270(94)90144-9.

STAR★METHODS

KEY RESOURCES TABLE

REAGENT or RESOURCE	SOURCE	IDENTIFIER
Antibodies		
Rabbit Anti-c-Fos antibody	Synaptic Systems	Cat#226003; RRID: AB_2231974
Anti-Calcitonin Gene Related Peptide antibody produced in rabbit	Sigma	Cat#C8198; RRID: AB_259091
Anti-Neurofilament 200 antibody produced in rabbit	Sigma	Cat#N4142; RRID: AB_477272
NeuN Polyclonal antibody	Proteintech (China)	Cat#26975-1-AP; RRID: AB_2880708
Anti-Tyrosine Hydroxylase Antibody	Millipore	Cat#AB152; RRID: AB_390204
Sheep Anti-Digoxigenin Fab fragments Antibody, AP Conjugated	Roche	Cat#11093274910; RRID: AB_514497
isolectin GS-IB4 from *Griffonia simplicifolia*, Alexa Fluor® 568 conjugate	Thermo Fisher Scientific	Cat#I21412; RRID: N/A
Alexa Fluor(R) 594 anti-Tubulin Beta 3 (TUBB3) antibody	BioLegend	Cat#657408; RRID: AB_2565285
Alexa Fluor 488-AffiniPure Goat Anti-Rabbit IgG (H+L)	Jackson ImmunoResearch Labs	Cat#111-545-003; RRID: AB_2338046
Alexa Fluor 594-AffiniPure Goat Anti-Rabbit IgG (H+L) antibody	Jackson ImmunoResearch Labs	Cat#111-585-003; RRID: AB_2338059
Goat Anti-Rabbit IgG H&L (Alexa Fluor 647) preadsorbed antibody	Abcam	Cat#ab150083; RRID: AB_2714032
Bacterial and virus strains		
rAAV-EF1α-DIO-hM3D(Gq)-mCherry-WPREs	BrainVTA	Cat#PT-0042
rAAV-EF1α-DIO-mCherry-WPRE-pA	BrainVTA	Cat#PT-0013
rAAV-VGLUT2-CRE-WPRE-hGH-pA	BrainVTA	Cat#PT-2592
rAAV-EF1α-DIO-EYFP-WPRE-hGH-pA	BrainVTA	Cat#PT-0012
Chemicals, peptides, and recombinant proteins		
Tamoxifen	APExBIO, Houston, USA	Cat#B5965; CAS: 10540-29-1
Clozapine N-oxide(CNO)	APExBIO, Houston, USA	Cat#A3317; CAS: 34233-69-7
Diphtheria Toxin from *Corynebacterium diphtheriae*	Sigma	Cat#D0564; CAS: N/A
Tetrodotoxin	Chengdu Must Bio-Technology Co.,Ltd	Cat#A0224; CAS: 4368-28-9
Strychnine	Sigma	Cat#S0532; CAS: 57-24-9
Bicuculline	Sigma	Cat#14343; CAS: 40709-69-1
DIG RNA Labeling Mix	Roche	Cat#11277073910; CAS: 186033-10-3
Experimental models: Organisms/strains		
Mouse: STOCK Mrgprd<tm1.1(cre/ERT2)Wql>/J	Jackson Laboratory	JAX: 031286; RRID: IMSR_JAX:031286
Mouse: B6.Cg-Gt(ROSA)26Sor/J	Jackson Laboratory	JAX: 024109; RRID: IMSR_JAX:024109
Mouse: C57BL/6-Gt(ROSA)26Sor/J	Jackson Laboratory	JAX: 007900; RRID: IMSR_JAX:007900
Software and algorithms		
GraphPad Prism 9	GraphPad	RRID: SCR_002798
pClamp 10.6	Molecular Devices	RRID: SCR_011323
Fiji	Fiji	RRID: SCR_002285
FV31S-SW Viewer	Olympus	https://www.olympus-lifescience.com

RESOURCE AVAILABILITY

Lead contact

Further information and requests for resources and reagents should be directed to and will be fulfilled by the lead contact, Yan Zhang (yzhang19@ustc.edu.cn).

Materials availability

This study did not generate new unique reagents.

Data and code availability

- All data reported in this paper will be shared by the lead contact upon request.
- This paper does not report original code.
- Any additional information required to reanalyze the data reported in this paper is available from the lead contact upon request.

EXPERIMENTAL MODEL AND SUBJECT DETAILS

Animals

All animal experiments were performed with protocols approved by the Animal Care and Use Committee of the University of Science and Technology of China. Mice were maintained under a 12-h light/dark cycle (lights on from 07:00 to 19:00) at a stable temperature (23–25 °C) and with *ad libitum* access to water and food. The genetically modified mice, including *Mrgprd*^{CreERT2}, *ROSA*$^{ChR2\text{-}EYFP}$ (*Ai32*) and *ROSA26*^{iDTR} (*DTR*) mice, were purchased from Jackson Laboratories. *Mrgprd*^{CreERT2}; *ROSA*$^{ChR2\text{-}EYFP}$ mice (referred to as *Mrgprd*^{CreERT2}*-ChR2* mice) were generated by crossing *Mrgprd*^{CreERT2} mice with *ROSA*$^{ChR2\text{-}EYFP}$ mice. *Mrgprd*^{CreERT2}; *ROSA26*^{iDTR} mice (referred to as *Mrgprd*^{CreERT2}*-DTR mice*) were generated by crossing *Mrgprd*^{CreERT2} mice with *ROSA26*^{iDTR} mice. To label or manipulate adult Mrgprd-expressing neurons, we performed 5 consecutive daily intraperitoneal injections of tamoxifen (100 μl, 75 mg/kg) starting at P21 in *Mrgprd*^{CreERT2}, *Mrgprd*^{CreERT2}*-ChR2 and Mrgprd*^{CreERT2}*-DTR* mice. To ablate Mrgprd^{+} neurons, diphtheria toxin (DTX, 20 μg/kg) was injected intraperitoneally for 5 consecutive days in 6–8 weeks old *Mrgprd*^{CreERT2}*-DTR mice* (also referred to as Mrgprd-ablated mice). To study the role of Mrgprd^{+} neurons in the development of allodynia, SNI operation and behavioral test were performed 3 weeks after DTX injections. To study the role of Mrgprd^{+} neurons in the maintenance of allodynia, we ablated Mrgprd^{+} neurons after SNI (post-SNI, day 15–19). Littermates that lacked either the *ROSA26*^{iDTR} or *Mrgprd*^{CreERT2} allele but received the same diphtheria toxin injections were used as controls (*Mrgprd*^{CreERT2} or *DTR* mice). Both males and females were used. Animals were assigned to treatment groups randomly, and behavioral responses were measured in a blinded manner.

METHOD DETAILS

Spared nerve injury (SNI)

After anesthetization by 3% isoflurane, the left hindlimb was fixed in a lateral position. Using the femur as a reference point, cut the skin and separated the muscle with blunt glass needles. Then, the sciatic nerves with three peripheral branches (sural, common peroneal, and tibial nerves) were exposed. Tibial and common peroneal nerves were ligated with 4-0 silk and severed for a 1–2 mm section. The sural nerve was carefully preserved. Then, the skin is sutured and disinfected with iodophor. In the sham group, the sciatic nerve was exposed but not ligated and severed.

Von Frey test

All animals were habituated to the metal mesh containers (6.5 cm × 6.5 cm × 6 cm) placed on the perforated metal mesh floor (6.5 mm × 6.5 mm) before the mechanical hypersensitivity test. After three consecutive "habituation" sessions for 30 min per day, punctate mechanical sensitivity was measured by stimulating the plantar area of hind paws with a series of von Frey filaments with different strengths (g). Using Dixon's up-down method,[59] the thresholds inducing withdrawal responses were determined. Dynamic mechanical sensitivity was assessed by light stroking from heel to toe of the plantar area of hind paws using a paintbrush.[36] Fast movement, lifting the stimulated paw for less than 1 s was scored 0. Sustained lifting (more than 2 s) of the stimulated paw toward the body was scored 1; one strong lateral paw lift, above the level of the body or a startle-like jump was scored 2; and multiple flinching responses

or licking of the affected paw was scored 3. Three trials at 10 s intervals were performed, and an average score was noted for each mouse.

Hargreaves test

Thermal sensitivity was evaluated on the Hargreaves apparatus (Model390; IITC Life Science Inc, Woodland Hills, CA). Mice were placed in the clear arena on a glass with constant temperature (30 °C). After 60 min/d habituation for 3 consecutive days, the plantar surface of the hind paw was exposed to a beam of light (4 × 6 mm size, 25% of maximum intensity), and paw withdrawal latencies (PWL) were measured. Five trials were conducted for each animal with an interval of at least 5 min. The maximum and minimum PWL were excluded to minimize the variation, and the average of the remaining 3 trials was calculated for each mouse. A cutoff of 20 seconds was used to prevent tissue damage.

High-threshold von Frey filament-induced behaviors

To study the behavioral responses evoked by high-threshold von Frey filament (1.0 g), mice were placed on the perforated metal mesh floor (6.5 cm × 6.5 cm) for 30 min habituation before test. Mice then received ten separate mechanical stimuli (1.0 g) for 1–2 s with 3–5 s intervals at hindpaw. Paw lifting, licking and fluttering were analyzed. Lifting: raise paws instead of moving around, Licking: turn the head and lick the paw, Fluttering: rapid and repeated lifting.

To evaluate high-threshold mechanical force-evoked behaviors following ablation of *Mrgprd*^{CreERT2}-marked neurons, *Mrgprd*^{CreERT2} or *DTR* mice, *Mrgprd*^{CreERT2} or *DTR*&SNI mice, *Mrgprd*^{CreERT2}-*DTR*&SNI mice received stimuli after 30 min habituation.

To evaluate high-threshold mechanical force-evoked behaviors following chemogenetic activating *Mrgprd*^{CreERT2}-marked neurons, hM3Dq or mCherry-injected *Mrgprd*^{CreERT2} mice received stimuli 30 min after intraperitoneal (i.p.) injection of CNO (2 mg/kg).

Chemogenetics-induced behaviors

To study the behavioral responses evoked by chemogenetic activation of Mrgprd^{+} neurons, animals received i.p. injection of CNO (2 mg/kg). Then, animals were individually placed in a colorless acrylic chamber (100 mm × 100 mm × 100 mm). The lifting and licking behaviors after the CNO injection were recorded by Camera for 1 hour.

To study mechanical and thermal sensitivity following priming chemogenetic activation of Mrgprd^{+} neurons, hM3Dq or mCherry-injected *Mrgprd*^{CreERT2} mice received von Frey and Hargreaves tests at 0.5 h, 1 h, 2 h, 4 h and 6 h after i.p. injection of CNO (2 mg/kg).

To study the role of the ERK signaling pathway in Mrgprd-induced mechanical allodynia, the MEK inhibitor PD98059 (Sigma, 0.5 μg/10 μl) or vehicle (10 μl 10%DMSO in PBS) was intrathecally injected at 30 min before i.p. injection of CNO (2 mg/kg). Animals received von Frey and brush test after PD98059 injection and at 0.5 h, 1 h, 2 h, 4 h and 6 h after CNO injection.

Optogenetics-induced changes in mechanical and thermal sensitivity

To study the mechanical sensitivity following priming optogenetic activation of Mrgprd^{+} neurons, *Mrgprd*^{CreERT2}-*ChR2* mice were individually placed in a chamber (6.5 cm × 6.5 cm × 6 cm) with a hollow floor of wire. A 1 mm fiber (Inper) is connected to the laser (QAXK-LASER) to continuously stimulate the glabrous skin of the hindpaw at 10 Hz and 20 mW/mm^2 intensity for 10 min. Light intensity was measured by the laser power meter (LP1, Sanwa). Animals received von Frey and brush test at 0.5 h, 1 h, 2 h, 4 h and 6 h after termination of light stimulation.

Real-time place avoidance (RTPA) and conditioned place avoidance (CPA)

All animals were habituated to the custom-made apparatus for two consecutive days for 30 min per day before being subjected to a two-chamber RTPA or CPA test. The device size is 200 mm x 100 mm x 100 mm, and the device is divided into two chambers by a partition with a hole (40 mm x 40 mm) in the middle. The two chambers have distinct stripe patterns.

RTPA

RTPA test consists of the pre-stimulation phase (10 min), stimulation phase (10 min) and post-stimulation phase (10 min). During the pre-stimulation phase, mice were allowed to move freely between two chambers. The time spent in each chamber was calculated, and the preferred chamber was determined before stimulation. During the stimulation phase, once the mice entered the preferred chamber, corresponding stimuli (von Frey filament, brush, or light) were applied to the mice's hindlimb. In the post-stimulation phase, the mouse explored two chambers again without stimulation. The time spent in the preferred chamber was recorded.

To evaluate low-threshold mechanical force-induced aversion following SNI in Mrgprd-ablated mice, the RTPA test was carried out 14 days after SNI. The von Frey filaments (0.16 g or 0.4 g) and brush were used during the stimulation phase.

To evaluate low-threshold mechanical force-induced aversion following chemogenetic activating Mrgprd^{+} sensory neuron, hM3Dq or mCherry-injected *Mrgprd^{CreERT2}* mice received i.p. injection of CNO (2 mg/kg) and returned to their home cages. RTPA test was carried out 20 min after injection. The von Frey filaments (0.16 g or 0.4 g) and brush were used during the stimulation phase.

To evaluate low-threshold mechanical force-induced aversion following hindpaw transdermal blue/yellow light stimulation in *Mrgprd^{CreERT2}-ChR2* mice, 10 min blue or yellow light (10 Hz, 20 ms pulse-width, 20 mW/mm^2) was applied to hindpaw. RTPA was carried out 20 min later. The von Frey filaments (0.16 g or 0.4 g) and brush were used during the stimulation phase.

CPA

The CPA experiment lasted for 4 days and was divided into the pre-stimulation phase (day 1), stimulation phase (day 2 and day 3), and post-stimulation phase (day 4). Time spent in each chamber was calculated, and the preferred chamber was determined on day 1. On day 4, time spent in the preferred chamber within 10 min was recorded.

For chemogenetic activation-induced CPA, hM3Dq or mCherry-injected *Mrgprd^{CreERT2}* mice moved freely on day 1 and day 4. On day 2 and day 3, mice received i.p. injection of CNO (2 mg/kg) and were restricted to the preferred chamber for 1 hour.

Intrathecal virus injection

Intrathecal injections were performed in mice at the L5 and L6 intervertebral spaces. Briefly, six-week-old *Mrgprd^{CreERT2}* mice were continuously anesthetized by isoflurane and a volume of 10 μl rAAV-EF1α-DIO-hM3D(Gq)-mCherry-WPREs (5.54E+13 vg/ml, BrainVTA, PT-0042, diluted 1:10 in PBS) was injected for chemogenetic manipulation with a Hamilton microsyringe. The rAAV-EF1α-DIO-mCherry-WPRE-pA (5.19E+13 vg/ml, BrainVTA, PT-0013, diluted 1:10 in PBS) was used as the control. Puncture of the dura was indicated behaviorally by a flick of the tail. After the injection, the needle was maintained for an additional 30 s. Behavioral tests were performed 21 days later.

Intraspinal stereotaxic injection

The intraspinal injection was performed at the spinal segments between T12–T13 and T13–L1 vertebrae to target neurons in L3–L6 spinal segments. To label excitatory neurons, the blended virus was prepared by mixing rAAV-VGLUT2-CRE-WPRE-hGH-pA (5.13E+12 vg/ml, BrainVTA, PT-2592) with rAAV-EF1α-DIO-EYFP-WPRE-hGH-pA (5.24E+12 vg/ml, BrainVTA, PT-0012) uniformly with the ratio of 1:1 (v/v). Mice were anesthetized using 3% isoflurane and fixed in stereotaxic apparatus by the mouse spinal adaptor (RWD Life Science, China). The T12–T13 vertebral junction was located near the peak of the hump. After removing the muscles and ligaments, the lumbar spinal cord and central dorsal blood vessel were exposed. The virus was injected at 500 μm laterally to the central dorsal blood vessel and at a depth of 400 μm. By using the glass microelectrode, 400 nl of virus was injected at a rate of 30 nl/min per point. After the injection, the glass microelectrode was maintained for an additional 5 min. The electrophysiological recording was performed 2 weeks after virus injection.

Immunofluorescence (IF) and *in situ* hybridization (*ISH*)

Animals were anesthetized by 3% isoflurane and intracardially perfused with 20 ml 1×DEPC-treated PBS (4 °C) followed by 20 ml DEPC-treated paraformaldehyde (PFA) (4°C). Brain, spinal cord (L3–L5) and DRG (L3–L5) were removed and post-fixed by 4% DEPC-treated PFA for an additional 12 h at 4°C and dehydrated by 30% sucrose. After dehydration, tissues were embedded in OCT (SAKURA, 4583) and sectioned (spinal cord 25 μm, DRG 15 μm) by a cryostat (Leica CM1950).

IF

For immunofluorescence, frozen sections were washed 3 times for 5 min with 1×PBS before being permeabilized in 0.4% Triton X-100 (Sangon Biotech, A110694) (in PBS) for 15 min. To block the non-specific antibody binding, the sections were incubated in 10% normal goat serum (Absin, abs933) (in PBST) for 1 hour and then incubated with primary antibody (rabbit anti-c-Fos antibody, 1:1000, Synaptic Systems, Cat# 226003; rabbit anti-CGRP antibody, 1:1000, Sigma, Cat# C8198; Alexa-568-conjugated IB4, 1:1000, Thermo Fisher Scientific, Cat# I21412; anti-Tubulin Beta3 antibody, 1:1000, BioLegend, Cat# 657408; rabbit anti-NF200 antibody, 1:1000, Sigma, Cat# N4142; rabbit anti-NeuN antibody, 1:200, Proteintech, Cat# 26975-1-AP; rabbit anti-TH antibody, 1:1000, Millipore, Cat# AB152) overnight at 4 °C. The sections were then washed 3 times for 5 min in PBST and then incubated with the secondary antibody (Alexa Fluor 488-AffiniPure Goat Anti-Rabbit IgG (H+L), 1:500, Jackson, Cat# 111-545-003; Alexa Fluor 594-AffiniPure Goat Anti-Rabbit IgG (H+L) antibody, 1:500, Jackson, Cat# 111-585-003; Goat Anti-Rabbit IgG H&L (Alexa Fluor 647) preadsorbed antibody, 1:500, Abcam, Cat# ab150083) for 1 hour at room temperature. Next, the sections were washed 3 times for 5 min in PBS and mounted on slides. Images were taken with confocal microscopes (FV3000, Olympus).

ISH

The *Mrgprd*-RNA probe was designed based on the online *in situ* hybridization data (https://mousespinal.brain-map.org/imageseries/detail/100039689.html). The *in situ* hybridization was performed using *Mrgprd*-RNA probe labeled with Anti-Digoxigenin-AP (Roche, Cat# 11093274910).

On day 1, the slides with DRG slices were baked at 55°C for 30 min followed by 20 min fixation in 4% DEPC-PFA. Slides were then washed in DEPC-PBS for 5 min (2 times) and treated with 1 ng/μl proteinase K (Roche, Cat# 3115879001) in PK buffer (5% 1 M DEPC-Tris-HCl, 1% 0.5 M EDTA, 0.15% 1 ng/μl PK, 94% DEPC-ddH_2O) for 3 min, and washed in DEPC-PBS for 5 min. After refastened with 4% DEPC-PFA for 10 min and washed in DEPC-H_2O for 5 min (2 times), we added 0.1 M RNase-free triethanolamine-HCl (pH 8.0) with 0.25% acetic anhydride to incubate the tissue for 10 min and washed in DEPC-PBS for 5 min. The tissues were then prehybridized for 1 hour at room temperature in pre-hybridization buffer (50% formamide, 25% 5×SSC, 0.3 mg/ml yeast RNA, 0.1 mg/ml heparin, 1 × Denhardt's, 0.1% Tween-20, 5 mM EDTA) and replaced with 1–2 μg/ml of the probe in hybridization buffer and continued the incubation at 65°C for 12–16 hours.

On day 2, the slides were washed in pre-warmed (65 °C) 2 × SSC buffer (Sangon Biotech, B548110), then added RNase A (3 μg/ml) in 37°C 2 × SSC for 30min. Next, slides were washed in 2 × SSC at 65°C for 30 min and in PBT at room temperature for 10 min (2 times). Tissues were then blocked (10% heat-inactivated sheep serum in PBT) and incubated in antibody (diluted 1:1000 in PBT and 10% sheep serum) overnight at 4°C.

On day 3, the slides were washed in PBST for 20 min (3 times) and in AP buffer (1 M Tris pH = 9.5, 5 M NaCl, 10% Triton 100) for 5 min. Then the slides were dipped in a buffer (0.0012 g/ml levamisole in AP buffer) for 5 min. The sections were visualized in buffer containing NBT (75 mg/ml) and BCIP (50 mg/ml). The ISH images were converted to pseudo colors and merged by Fiji software.

c-Fos induction

To study c-Fos expression by von Frey filaments in the spinal cord, background c-Fos fluorescence was minimized by placing mice in the training apparatus for a period of 4 hours before treatment. And then, the hindpaw was stimulated for 10 min by von Frey (0.16 g). After the stimulation, mice were allowed to move freely in the apparatus for an additional 1.5 hours and sacrificed. Spinal cord was excised for immunofluorescence analysis.

Cell counting

The fluorescence cells were counted by Olympus Confocal microscopy (FV3000). The number of Mrgprd$^+$ neurons detected by *in situ* hybridization was counted by ImageJ (Fiji). Density was calculated via dividing the number of Mrgprd$^+$ neurons by the total DRG cell area.

Spinal cord slice electrophysiology

Spinal cord slice preparation

Parasagittal spinal cord slices with attached dorsal roots (10–20 mm) and DRG were optimized according to previous studies.[28,36] Mice (8–13 weeks) were anesthetized with pentobarbital sodium (2% w/v, i.p.) and intracardially perfused with 25 ml ice-cold NMDG substituted artificial cerebrospinal fluid (NMDG-ACSF) containing (in mM) 93 N-methyl-d-glucamine (NMDG), 2.5 KCl, 1.2 NaH_2PO_4, 30 $NaHCO_3$, 20 HEPES, 25 glucose, 2 thiourea, 5 Na-ascorbate, 3 Na-pyruvate, 0.5 $CaCl_2$, 10 $MgSO_4$ and 3 glutathione (GSH). PH was titrated to 7.3–7.4 with HCl, and osmolarity was 310–320 mOsm. The lumbar spinal cord was quickly removed to ice-cold oxygenated NMDG-ACSF, and the spinal cord with full-length dorsal root and DRG attached was cut on a vibratome (VT1200S, Leica), as illustrated in Figures 3A and S4A. To study the Aβ--fibers pathway in mediating allodynia, we prepared Aβ-input preparation (Figure 3A). To study the C-fibers pathway in mediating mechanical hyperalgesia, low-threshold Aβ-fiber inputs to dorsal horn neurons were eliminated by moving the second cut more laterally (Figure S4A). The spinal cord slices were initially incubated in NMDG-ACSF for 10 min at 32°C, followed by N-2-hydroxyethylpiperazine-N-2-ethanesulfonic acid (HEPES) ACSF containing (in mM) 92 NaCl, 2.5 KCl, 1.2 NaH_2PO_4, 30 $NaHCO_3$, 20 HEPES, 25 glucose, 2 thiourea, 5 Na-ascorbate, 3 Na-pyruvate, 2 $CaCl_2$, 2 $MgSO_4$ and 3 GSH (pH 7.3–7.4, 310–320 mOsm, oxygenated with 95% O_2 and 5% CO_2) for more than 1 h at 25°C. Slices were then transferred to a recording chamber and continuously perfused with standard recording ACSF at 3–5 ml/min at 32°C.

Patch-clamp recordings and dorsal root stimulation

Whole-cell recording experiments were performed as described previously.[28,36] Recordings were made from randomly picked neurons in the laminae I-II$_o$ and $_v$II$_i$ using oxygenated recording ACSF containing (in mM) 125 NaCl, 2.5 KCl, 2 $CaCl_2$, 1 $MgCl_2$, 1.25 NaH_2PO_4, 26 $NaHCO_3$, 25 d-glucose, 1.3 sodium ascorbate and 3.0 sodium pyruvate, with pH at 7.3 and measured osmolality at 310–320 mOsm. The internal solution contains (in mM): potassium gluconate 130, KCl 5, Na_2ATP 4, NaGTP 0.5, HEPES 20, EGTA 0.5, pH 7.28 with KOH, and measured osmolality at 310–320 mOsm. Data were acquired with pClamp 10.0 software using MultiClamp 700B patch-clamp amplifier (Molecular Devices) and Digidata 1550B (Molecular Devices). Responses were low-pass filtered on-line at 2 kHz and digitized at 5 kHz.

25 μA (pulse widths 0.1 ms) and 500 μA (pulse widths 0.1 ms) were used to screen Aβ fiber and C-fiber-mediated synaptic inputs/outputs of the spinal dorsal horn neurons. The distance from the tip of the stimulation electrode to the entrance of the attached dorsal root is around 10 mm. 473 nm blue light (20 ms) was used to screen Mrgprd$^+$ fiber-mediated synaptic inputs of the spinal dorsal horn neurons in *Mrgprd^{CreERT2}-ChR2* mice. To record dorsal root stimulation-evoked excitatory postsynaptic currents (eEPSCs), membrane potential was held hold at -70 mV to attenuate evoked inhibitory postsynaptic currents (eIPSCs), such that even small eEPSCs could be detected. By holding the membrane potential at -45 mV, eIPSCs can be detected. To record dorsal root stimulation-evoked EPSPs/APs (Aβ and C-eEPSPs/eAPs), current-clamp recordings were performed at the resting membrane potential; for neurons with spontaneous firing, the hyperpolarizing current was injected to unmask synaptic responses. The recordings were performed either under the normal recording solution or under the disinhibition condition by adding bicuculline (10 μM) and strychnine (2 μM) to ACSF. To record sEPSCs, the neurons were held at -70 mV after establishing the whole-cell configuration and the data were analyzed with Mini Analysis. To test the influences of chemogenetic activation of *Mrgprd^{CreERT2}* neurons on Aβ-eEPSCs/APs, C-eEPSCs/APs, A currents and D currents, mice were sacrificed for electrophysiological recording at one hour after i.p. injection of CNO (2 mg/kg). To test the effect of optogenetic activation of Mrgprd$^+$ neurons on Aβ-eEPSCs/APs and C-eEPSCs/APs, the glabrous skin of hindpaw in *Mrgprd^{CreERT2}-ChR2* mice was continuously stimulated for 10 min (10 Hz, 20 ms pulse-width, 20 mW/mm^2) and then mice were sacrificed for electrophysiological recording 30 min later.

To assess the firing pattern of neurons, membrane potential was held at -85 mV to prevent the inactivation of the potassium channel. The firing pattern was examined by 1000 ms depolarizing step current injection range from 15 pA to 225 pA. The delayed firing pattern was characterized by a prominent delay between the onset of the depolarizing step and the AP discharge. The latency to first AP firing following the current

injection was determined between the current injection onset and the AP peak. The neurons without AP following 225 pA current injection were excluded from the analysis of the latency to first AP.

Monosynaptic Mrgprd$^+$-fiber inputs were identified by the absence of failures in response to 5 stimuli at 1 Hz, and jitter of L-eEPSCs latencies in response to 7 stimuli at 0.05 Hz less than 2 ms.[41]

I_A and I_D recording

The recording solution for I_A recording is Ca^{2+}-free ACSF containing (in mM) 80 NaCl, 2.5 KCl, 1.25 NaH_2PO_4, 3 $MgCl_2$, 25 $NaHCO_3$, 75 sucrose, 1.3 sodium ascorbate, 3.0 sodium pyruvate and 0.5 μM TTX (tetrodotoxin) to block voltage-gated Na^+ currents, Ca^{2+} currents and Ca^{2+}-activated K^+ currents. The capacitance and series resistance were well compensated. To record I_A, a two-step voltage protocol was used, as illustrated in Figure 7E. The first step was to record the total outward current (I_A+I_D), and voltage steps of 500 ms pulses stepping from -80 mV to +40 mV were applied at 5 s intervals. To determine the I_D, conditioning 150 ms pre-pulses ranging from -80 mV to -10 mV were applied to inactivate transient potassium channels and then followed by a step to +40 mV for 500 ms at 5 s intervals. Subtraction of the I_D from the total current isolated the I_A. Series resistances for all neurons recorded in this study were within 30 MΩ.

DRG neurons electrophysiology

DRG neurons culture

Mouse spinal columns were removed and dissected on the ice. DRGs were acutely dissociated and placed in DH10 medium (90% DMEM/F-12, 10% Fetal Bovine Serum, 100 U/ml penicillin, 100 μg/ml streptomycin, Gibco). After removing the supernatant, DRGs were transferred in 1 ml digestive enzymes containing 1 ml 2.5% trypsin and 1 mg collagenase type I (Gibco) and then incubated at 37°C for 45 min. After digestion, DRG neurons were scattered and suspended in DH10 medium, then plated on 6 mm coverslip coating with 0.5 mg/ml poly-D-lysine (Sigma) and 10 μg/ml laminin (Gibco). Then they were cultured in an incubator at 37°C for 1 hour, and DH10 medium with 20 ng/μl nerve growth factor (Sigma) was added. These neurons were used for electrophysiological recordings 2 hours later.

DRG neurons patch-clamp recordings

Whole-cell recording experiments were performed as spinal cord neurons. The recording was made from mCherry$^+$ or EYFP-ChR2$^+$ neurons identified by fluorescence microscope (Olympus) using oxygenated ACSF containing (in mM) 140 NaCl, 4 KCl, 2 $CaCl_2$, 2 $MgCl_2 \cdot 6H_2O$, 10 HEPES, 5 glucose (pH 7.4, oxygenated with 95% O_2 and 5% CO_2). The internal solution contains (in mM): 135 KCl, 1.1 $CaCl_2$, 2 EGTA, 3 Mg^{2+}-ATP, 0.5 Na^+-ATP (pH 7.4, adjusted by NaOH).

QUANTIFICATION AND STATISTICAL ANALYSIS

Data are expressed as the mean ± SEM except for the I_A/I_D current density and AP firing latency which are expressed as median with interquartile range (Q1–Q3 with median denoted in between). Statistical analysis was performed by GraphPad Prism. Normality was assessed using the Shapiro-Wilk test. When normally distributed, the data were analyzed with paired t-tests, unpaired t-tests as appropriate. When normality was violated, the data were analyzed with Wilcoxon signed-rank test for paired test and Mann-Whitney *U* test for unpaired test. For RTPA and CPA, data were subject to paired Student's t tests or Wilcoxon signed-rank test. For *ISH*, DRG cells counting, 1.0 g von Frey-evoked paw licking and membrane potential assessment following chemogenetic and optogenetic activation of Mrgprd$^+$ neurons, amplitude, latency to first AP, data were subjected to unpaired Student's t tests or Mann-Whitney *U* tests. For c-Fos counting and 1.0 g von Frey-evoked behaviors, data were assessed by One-way ANOVA with holm-sidak test. For SNI-induced mechanical and thermal hypersensitivity changes following ablation of Mrgprd$^+$ neurons, thermal and mechanical sensitivity changes following chemogenetic and optogenetic activation of Mrgprd$^+$ neurons, SNI-induced changes in the excitability of Mrgprd$^+$ neurons, data were assessed by Two-way repeated-measures ANOVA with holm-sidak test. For statistical analysis of the incidence of electrophysiological results, data were analyzed with chi-square tests. $p < 0.05$ was considered as a significant change.